
Identifiable Steering via Sparse Autoencoding of Multi-Concept Shifts

Shruti Joshi^{1 2} Andrea Dittadi^{3 4 5} Sébastien Lachapelle⁶ Dhanya Sridhar^{1 2}

Abstract

Steering methods manipulate the representations of large language models (LLMs) to induce responses that have desired properties, e.g., truthfulness, offering a promising approach for LLM alignment without the need for fine-tuning. Traditionally, steering has relied on supervision, such as from contrastive pairs of prompts that vary in a single target concept, which is costly to obtain and limits the speed of steering research. An appealing alternative is to use unsupervised approaches such as sparse autoencoders (SAEs) to map LLM embeddings to sparse representations that capture human-interpretable concepts. However, without further assumptions, SAEs may not be identifiable: they could learn latent dimensions that entangle multiple concepts, leading to unintentional steering of unrelated properties. We introduce Sparse Shift Autoencoders (SSAEs) that instead map the *differences* between embeddings to sparse representations. Crucially, we show that SSAEs are identifiable from paired observations that vary in *multiple unknown concepts*, leading to accurate steering of single concepts without the need for supervision. We empirically demonstrate accurate steering across semi-synthetic and real-world language datasets using Llama-3.1 (Llama Team et al., 2024) embeddings.

1. Introduction

As increasingly powerful large language models (LLMs) are deployed and widely used, researchers seek to *steer* their behaviour at inference time, without the need to perform expensive model updates, as with fine-tuning. Steering refers to perturbing an LLM’s representation of an input prompt (potentially at different layers in the LLM) so that the LLM responds with some desired property. For example, recent

work has estimated steering vectors for sycophancy (Rimsky et al., 2024), sentiment (Subramani et al., 2022), machine unlearning (Li et al., 2024b), and even exploration in the case of LLM agents (Rahn et al., 2024). As such, research that improves the ease of steering has the potential to impact the alignment of LLMs to human values, such as harmlessness and helpfulness. However, a crucial assumption made by related work is access to supervision, either from target responses to prompts (c.f., Subramani et al. (2022)), or from contrastive pairs of prompts that differ by a single target concept like truthfulness (c.f., Turner et al. (2024); Rimsky et al. (2024)). Since supervision is costly, designing steering methods that can learn with limited supervision that is easily accessible, could speed up steering research. To this end, this paper focuses on learning to steer from paired samples that vary in multiple unknown concepts.

To better understand the challenges with unsupervised learning, consider a naive approach to learn to steer: obtain a dataset of *LLM embeddings of text* and to this data, fit an autoencoder that learns to map LLM embeddings to some latent space and decode the original vectors back. Assuming the learned latent space captures human-interpretable concepts, steering involves encoding an embedding, perturbing a single dimension in the latent space, and decoding to obtain the steered embedding. This example of an unsupervised approach is a simplified version of existing approaches to interpreting LLMs using sparse autoencoders (Cunningham et al., 2023). Why might this unsupervised approach fail to output accurate steered embeddings? The problem is that by fitting observations alone, autoencoders are generally not *identifiable*: infinitely many encoders and decoders can fit the observations equally well. In the context of steering, this means that in general the learned latent space does not capture individual concepts but rather some nonlinear entangling¹ thereof so that sparse latent perturbations steer multiple concepts at once and not the target concept alone.

In contrast to the naive unsupervised learning approach, the field of causal representation learning (CRL) proposes numerous approaches to identifiable generative models (see Section 4 for related work). However, these approaches focus on generative models of low-level data such as im-

¹Université de Montréal ²Mila - Quebec AI Institute ³Helmholtz AI ⁴Technical University of Munich ⁵MPI for Intelligent Systems, Tübingen ⁶Samsung - SAIT AI Lab, Montreal. Correspondence to: Shruti Joshi <shrutijoshi98@gmail.com>.

¹Commonly referred to as polysemanticity (Bricken et al., 2023).

ages or text, and assume that the generative model can be inverted to perfectly recover the latent variables from the observations.² However, in the setting we study here, the space of latent concepts is much higher-dimensional than the space of LLM representations, making it impossible to invert the mapping from concepts to LLM representations. As an important step in bridging the gap between CRL and LLMs, [Rajendran et al. \(2024\)](#) formalize concepts as linear subspaces of an LLM’s representation, and identify a fixed number of desired concepts up to linear transformations using multiple concept-conditional datasets. In the context of steering, this has two implications: i) since concepts are linearly encoded by LLMs, to steer, we can simply add the same steering vector per concept, and ii) we could develop unsupervised approaches that only linearly entangle concept-specific steering vectors. We could learn to linearly unmix these vectors with supervision from paired samples varying by a single concept, but potentially from fewer samples than existing steering approaches since learning a linear function is all that is needed. However, the need for curated data remains a hindrance.

In this paper, we propose Sparse Shift Autoencoders (SSAEs), models that learn steering vectors from paired samples that vary in multiple unknown concepts. Such samples are cheap to obtain, for example, by pairing posts and their replies on a social media site. Briefly, the model maps embedding differences between samples in a pair to a latent space that reflects the concept changes and uses a linear decoding function to reconstruct the difference vector, following the *linear representation hypothesis* ([Mikolov et al., 2013](#); [Jiang et al., 2024](#)) in assuming that concepts are linearly encoded by LLMs. Crucially, we constrain the latent representation to be sparse, meaning that each example is modeled using as few concept changes as necessary. We then leverage the results developed by [Lachapelle et al. \(2023\)](#) and [Xu et al. \(2024\)](#) to prove that the proposed SSAE approach identifies *some* concepts, for which we can readily extract steering vectors. We study the SSAE empirically both with synthetic data, and with Llama-3.1 embeddings on several language datasets, finding that our proposed approach enables accurate steering using multi-concept changes, without the need for careful supervision.

Connection to sparse autoencoders. The SSAE approach that we theoretically analyze in this paper resembles sparse autoencoders (SAEs), models used to find interpretable features in LLM representations ([Cunningham et al., 2023](#); [Templeton et al., 2024](#)). However, SAEs build on sparse dictionary learning ([Stephane, 1999](#); [Mairal et al., 2009](#)), an idea from signal processing that factorizes signals into a sparse linear combination of vectors from a *much higher*

²In other words, the mapping from latents to observations is injective.

dimensional basis than the signal itself. While SAEs model the high-dimensional space of concepts, this comes at the cost of identifiability since inverting the observations to capture concepts is impossible. By contrast, here, we focus on concepts that naturally vary across data pairs, making identifiability analysis possible.

In sum, this work: 1) formalizes the problem of learning steering vectors from multi-concept data from the lens of identifiability; 2) proposes the SSAE to model multi-concept shifts and establishes identifiability guarantees for these models based on sparsity regularization; 3) demonstrate the usefulness of the SSAE method for steering Llama-3.1 embeddings on both semi-synthetic and real language datasets, establishing a useful baseline for future work on tuning the behaviour of LLMs at inference time.

2. Identifiable learning of steering vectors

We begin by formalizing steering before developing a theory about learning steering vectors from multi-concept changes. Lowercase bold letters (\mathbf{x}) denote vectors, uppercase bold letters (\mathbf{A}) denote matrices, sets are denoted using uppercase letters (S) or calligraphic letters \mathcal{S} when they refer to domains of random variables. Please refer to [Apx. A.1](#) for notation followed in the paper.

2.1. Preliminaries

We assume that the observed data consists of vectors $\mathbf{x} \in \mathcal{X} \subseteq \mathbb{R}^{d_x}$ generated from underlying *concept representations* $\mathbf{c} \in \mathcal{C} \subseteq \mathbb{R}^{d_c}$ through an unknown generative process $g : \mathcal{C} \rightarrow \mathcal{X}$. Each data point \mathbf{x} is produced by a corresponding ground-truth concept representation \mathbf{c} such that $\mathbf{x} = g(\mathbf{c})$, where each component c_k corresponds to some abstract concept such as the language a text might be written in or its overall sentiment. While we cannot observe the concept representation \mathbf{c} of an observation \mathbf{x} , we have access to *learned representations* $\mathbf{z} = f(\mathbf{x})$, where the function $f : \mathcal{X} \rightarrow \mathcal{Z} \subseteq \mathbb{R}^{d_z}$ maps observations \mathbf{x} to d_z -dimensional real vectors $\mathbf{z} \in \mathcal{Z}$, known as their *embeddings*. For example, $f(\mathbf{x})$ can be learned via next-token prediction as with LLMs. However, there is no guarantee that $f = g^{-1}$ (the function g might not even be invertible). Consequently, true concept representations \mathbf{c} are *encoded* in the representations \mathbf{z} through the unknown composite function $\mathbf{z} = f(g(\mathbf{c}))$.

2.2. Problem formulation

In this paper, we are interested in learning *steering functions* that ideally allow us to manipulate the concepts that are represented in an observation such as a text. To directly manipulate concept k in the space \mathcal{C} ,³ we define the per-

³Such a space is also referred to as the privileged basis in interpretability literature ([Elhage et al., 2022](#)).

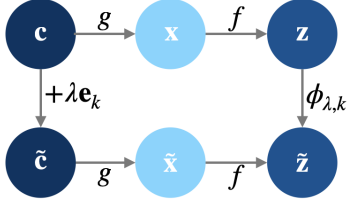


Figure 1: A steering function $\phi_{\lambda,k}$ is s.t. the above diagram commutes, i.e., $\phi_{\lambda,k}(f(g(\mathbf{c}))) = f(g(\mathbf{c} + \lambda\mathbf{e}_k)) \forall \mathbf{c}$. (see Defn. 1).

turbed concept vector as $\tilde{\mathbf{c}}_{k,\lambda} := \mathbf{c} + \lambda\mathbf{e}_k$, where \mathbf{e}_k is the k -th standard basis vector. The corresponding perturbed observation is $\tilde{\mathbf{x}}_{k,\lambda} := g(\tilde{\mathbf{c}}_{k,\lambda})$.

Definition 1. (Steering function) Fix a target concept k and $\lambda \in \mathbb{R}$. A **steering function** $\phi_{k,\lambda} : \mathcal{Z} \rightarrow \mathcal{Z}$ is a function such that for all $\mathbf{c} \in \mathcal{C}$, $\phi_{k,\lambda}(f(g(\mathbf{c}))) = f(g(\mathbf{c} + \lambda\mathbf{e}_k))$.

According to Defn. 1, a steering function maps each representation $\mathbf{z} = f(\mathbf{x})$ to its perturbed analog $\tilde{\mathbf{z}}_{\lambda,k} := f(\tilde{\mathbf{x}}_{\lambda,k})$, as illustrated in Figure 1. For example, if the k -th concept is language, a steering function maps $\mathbf{z} = f(\mathbf{x})$, the embedding of a sentence \mathbf{x} , to $\tilde{\mathbf{z}}_{k,\lambda} = f(\tilde{\mathbf{x}}_{k,\lambda})$, the embedding of the same sentence written in a different language. Although the change in \mathbf{c} is linear and sparse (only concept k is perturbed), the resulting change in \mathbf{z} might be nonlinear and dense. Steering functions are not guaranteed to exist. However, if f and g are injective, we have $\phi_{\lambda,k}(\mathbf{z}) = f(g(g^{-1}(f^{-1}(\mathbf{z})) + \lambda\mathbf{e}_k))$.

2.3. Learning steering vectors via multi-concept shifts

In practice, a steering function $\phi_{\lambda,k}$ can be learned via supervised learning given a dataset comprising of carefully designed paired observations $(\mathbf{x}, \tilde{\mathbf{x}}_k)$, in which a single concept changes between \mathbf{x} and $\tilde{\mathbf{x}}_k$ (Shen et al., 2017; Turner et al., 2024; Rimsky et al., 2024). However, such a dataset might be difficult to acquire. This raises the following question, at the heart of our contribution:

How can we learn a steering function $\phi_{k,\lambda}$ with a dataset of paired observations $(\mathbf{x}, \tilde{\mathbf{x}})$ in which multiple concepts vary?

Data-generating process. Following Locatello et al. (2020b), we consider paired observations $(\mathbf{x}, \tilde{\mathbf{x}})$ assumed to be sampled from the following generative process:

$$S \sim p(S), \quad (\mathbf{c}, \tilde{\mathbf{c}}) \sim p(\mathbf{c}, \tilde{\mathbf{c}} \mid S), \quad (1)$$

$$\mathbf{x} := g(\mathbf{c}), \quad \tilde{\mathbf{x}} := g(\tilde{\mathbf{c}}), \quad (2)$$

where $S \subseteq \{1, \dots, d_c\}$ denotes the subset of concepts that vary between \mathbf{x} and $\tilde{\mathbf{x}}$. More precisely, $p(\mathbf{c}, \tilde{\mathbf{c}} \mid S)$ is such that, with probability one, $\mathbf{c}_k = \tilde{\mathbf{c}}_k$ for all $k \notin S$. We also define the difference vectors $\delta^z := f(\tilde{\mathbf{x}}) - f(\mathbf{x}) = \tilde{\mathbf{z}} - \mathbf{z}$ and $\delta^c := \tilde{\mathbf{c}} - \mathbf{c}$. To rephrase what we just said differently, we have that $\delta_k^c = 0$ for all $k \notin S$. Crucially, across each

pair of observations, an unknown set of concepts changes, allowing us to leverage paired data that is cheap to obtain, such as posts and their replies on social media sites.

Varying concepts. In what follows, it will be useful to define $V \subseteq \{1, \dots, d_c\}$ to be the set of *varying concepts*:

$$V := \bigcup_{S: p(S) > 0} S. \quad (3)$$

The set V thus contains the concepts that can change in a pair $(\mathbf{x}, \tilde{\mathbf{x}})$. Even though concepts outside V are assumed to remain fixed *within* a pair $(\mathbf{x}, \tilde{\mathbf{x}})$, they can still vary *across* pairs. Without loss of generality, assume that $V := \{1, \dots, |V|\}$.

Method. We propose Sparse Shift Autoencoders (SSAEs), models of difference vectors δ^z consisting of an affine encoder $r : \mathbb{R}^{d_z} \rightarrow \mathbb{R}^{|V|}$ and an affine decoder $q : \mathbb{R}^{|V|} \rightarrow \mathbb{R}^{d_z}$. The representation $r(\delta^z)$ predicts δ_V^c , i.e., the concept shifts corresponding to δ^z , with $\delta_V^c = (\delta_i^c)_{i \in V}$ the subvector of δ^c corresponding to the index set V . The decoder q then maps these shifts back to embedding differences $\hat{\delta}^z$. We train SSAEs to solve the following constrained problem:

$$(\hat{r}, \hat{q}) \in \arg \min_{r, q} \mathbb{E}_{\mathbf{x}, \tilde{\mathbf{x}}} [\|\delta^z - q(r(\delta^z))\|_2^2] \quad (4)$$

$$\text{s.t. } \mathbb{E}_{\mathbf{x}, \tilde{\mathbf{x}}} \|r(\delta^z)\|_0 \leq \beta, \quad (5)$$

where Eqn. (4) is the standard auto-encoding loss that encourages good reconstruction and Eqn. (5) is a regularizer that encourages the predicted concept shift vector $\hat{\delta}_V^c := \hat{r}(\delta^z)$ to be sparse. Then, we use \hat{q} to decode single concept shifts into steering vectors. Formally, we end up with a steering function of the form

$$\hat{\phi}_k(\mathbf{z}) := \mathbf{z} + \hat{q}(\mathbf{e}_k), \quad (6)$$

where \hat{q} is a solution to the above constrained problem.

To summarize, our method consists of two steps:

1. Solving the sparsity regularized problem of Eqns. (4) and (5) to get an encoder-decoder pair (\hat{r}, \hat{q}) .
2. Use the vectors $\hat{q}(\mathbf{e}_k)$ for all $k \in V$ as steering vectors for all concepts (these are the columns of the matrix representing \hat{q}).

Theoretical justification. In Section 2.4 we will show that, under suitable assumptions on the data-generating process and a suitable choice of β , the ℓ_0 -regularized problem of Eqns. (4) and (5) is guaranteed to learn a (\hat{r}, \hat{q}) such that $\hat{r}(\delta^z) = \mathbf{P}\mathbf{D}\delta_V^c$ where \mathbf{D} is an invertible diagonal matrix, \mathbf{P} is a permutation matrix. In other words, the learned representation $\hat{r}(\delta^z)$ can be related to the ground-truth concept shift vector δ_V^c (considering only the varying concepts V) via a permutation-scaling matrix. We will later see how sparsity regularization is crucial for this to happen. Although our theoretical analysis assumes the learned representation has

size $|V|$, we find in Apx. B.3 that, in practice, our method maintains a reasonable degree of identifiability when the representation size is larger than $|V|$.

Furthermore, Section 2.5 will show how this identifiability guarantee implies that the functions $\hat{\phi}_k(\mathbf{z}) := \mathbf{z} + \lambda\hat{q}(\mathbf{e}_k)$ are valid steering functions (Defn. 1) for concepts $k \in V$.

Implementation. Informed by empirical insights about SAEs (Bricken et al., 2023; Gao et al., 2024), we parameterize the encoder and decoder as

$$\hat{\delta}_V^c := r(\delta^z) := \mathbf{W}_e(\delta^z - \mathbf{b}_d) + \mathbf{b}_e; \quad (7)$$

$$\hat{\delta}^z := q(\hat{\delta}_V^c) := \mathbf{W}_d\hat{\delta}_V^c + \mathbf{b}_d. \quad (8)$$

Moreover, since the ℓ_0 -norm is non-differentiable, in practice we replace it by an ℓ_1 -norm leading to the following relaxed sparsity constraint:

$$\mathbb{E}_{\mathbf{x}, \bar{\mathbf{x}}} \|r(\delta^z)\|_1 \leq \beta. \quad (9)$$

We then approximately solve this constrained problem by finding a saddle point of its Lagrangian using the ExtraAdam algorithm (Gidel et al., 2020) as implemented by Gallego-Posada & Ramirez (2022). Apx. B.1.2 provides a detailed discussion of the benefits of constraints as opposed to penalty to regularize objectives. Appropriate normalization is crucial for enforcing sparsity using the ℓ_1 -norm. Further details, including other implementation aspects, are discussed in Section 3 and Apx. B.

2.4. Identifiability analysis

This section explains why we expect the representation learned in Eqn. (4) to identify the ground-truth concept shift vector δ_V^c up to permutation and rescaling. To do so, we first demonstrate that, under suitable assumptions, the learned representation $\hat{r}(\delta^z)$ identifies the ground-truth concept shift δ_V^c up to an invertible linear transformation when we do not use sparsity regularization. Second, we show that by adding sparsity regularization, the learned representation identifies δ_V^c up to permutation and element-wise rescaling.

First, we provide justification for assuming an affine encoder-decoder pair in Eqn. (4):

Assumption 1 (Linear representation hypothesis). *The generative process $g : \mathcal{C} \rightarrow \mathcal{X}$ and the learned encoding function $f : \mathcal{X} \rightarrow \mathcal{Z}$ are such that $f \circ g : \mathcal{C} \rightarrow \mathcal{Z}$ is linear, implying there exists a $d_z \times d_c$ real matrix \mathbf{A} such that:*

$$\mathbf{z} = f(g(\mathbf{c})) = \mathbf{A}\mathbf{c}. \quad (10)$$

The linear representation hypothesis (LRH) implies that the learned representation \mathbf{z} linearly encodes concepts. A long line of work provides evidence for this hypothesis (c.f. Rumelhart & Abrahamson (1973); Hinton et al. (1986);

Mikolov et al. (2013); Ravfogel et al. (2020b)). More recently, theoretical work justifies why linear properties could arise in these models (c.f. Jiang et al. (2024); Roeder et al. (2021); Marconato et al. (2024)). Section 4 provides a full list of related work, while Apx. A.5 provides an explanation of the equivalence between LRH’s different interpretations. Rajendran et al. (2024) also leverage the LRH in their work.

Since we expect $d_c \gg d_z$, we cannot assume \mathbf{A} to be injective. Fortunately, we do not need to make this assumption, thanks to the following decomposition. Let $\bar{V} := [d_c] \setminus V$ be the complement of V . Then:

$$\begin{aligned} \delta^z &= \mathbf{A}\delta^c = \mathbf{A}_V\delta_V^c + \mathbf{A}_{\bar{V}}\delta_{\bar{V}}^c \\ &= \mathbf{A}_V\delta_V^c, \end{aligned} \quad (11)$$

where we used the fact that $\delta_{\bar{V}}^c = 0$, by definition of V . Eqn. (11) can be thought of as a generative process for the difference vectors δ^z , as opposed to \mathbf{z} , as in Eqn. (10). An additional key advantage of Eqn. (11) against Eqn. (10) is that the matrix involved in it has potentially fewer columns, since $|V| \leq d_c$. This suggests that, instead of assuming \mathbf{A} is injective, we assume its submatrix \mathbf{A}_V is injective.

Assumption 2. *The matrix $\mathbf{A}_V \in \mathbb{R}^{d_z \times |V|}$ is injective.*

Note that this implies that $d_z \geq |V|$, i.e., \mathbf{z} has at least as many dimensions as there are varying concepts. This is feasible given that d_z is typically around 10^3 (e.g., in LLMs), supporting a large set of varying concepts V .

To prove linear identifiability, we will need one more assumption. Let Δ_V^c be the support of the random vector δ_V^c . We will require that this support is diverse enough so that its linear span is equal to the whole space $\mathbb{R}^{|V|}$.

Assumption 3. *$\text{span}(\Delta_V^c) = \mathbb{R}^{|V|}$.*

With these assumptions, we can show linear identifiability by reusing proof strategies that are now common in the literature on identifiable representation learning (Khemakhem et al., 2020a; Roeder et al., 2021; Ahuja et al., 2022; Xu et al., 2024).

Proposition 2 (Linear identifiability). *Suppose (\hat{r}, \hat{q}) is a solution to the unconstrained problem of Eqn. (4). Under Asm. 1 to 3, there exists an invertible matrix $\mathbf{L} \in \mathbb{R}^{|V| \times |V|}$ such that $\hat{q} = \mathbf{A}_V\mathbf{L}$ and $\hat{r}(\mathbf{z}) = \mathbf{L}^{-1}\mathbf{A}_V^+\mathbf{z}$ for all $\mathbf{z} \in \text{Im}(\mathbf{A}_V)$, where $\text{Im}(\mathbf{A}_V)$ is the image of \mathbf{A}_V .*⁴

We prove Prop. 2 in Apx. A.2. The result follows naturally from the linear representation hypothesis in Asm. 1, but requires Asm. 2 and 3 for a complete proof. Rajendran et al. (2024) prove a similar result, showing that linear subspaces of representations that represent concepts are linearly identified from concept-conditional observations.

⁴We might not have $\hat{r}(\mathbf{z}) = \mathbf{L}\mathbf{A}_V^+\mathbf{z}$ for $\mathbf{z} \notin \text{Im}(\mathbf{A}_V)$, since the behavior of \hat{r} is unconstrained by the objective outside the support of δ^z , i.e., outside $\text{Im}(\mathbf{A}_V)$.

Identifiability up to permutation and rescaling. To go from identifiability up to linear transformation to identifiability up to permutation and rescaling, we need to make further assumptions. Let \mathcal{S} be the support of the distribution $p(S)$, i.e., $\mathcal{S} := \{S \subseteq [d_c] \mid p(S) > 0\}$. The following is based on Lachapelle et al. (2023) and Xu et al. (2024).

Assumption 4 (Sufficient diversity of multi-concept shifts). *The following two conditions hold.*

1. (Sufficient support variability): *For every varying concept $k \in V$, we have*

$$\bigcup_{S \in \mathcal{S} \mid k \notin S} S = V \setminus \{k\} \quad \forall k \in V; \quad (12)$$

2. (Conditional distribution $\mathbb{P}_{\delta_{\mathcal{S}}^c|S}$ is continuous): *For all $S \in \mathcal{S}$, the conditional distribution $\mathbb{P}_{\delta_{\mathcal{S}}^c|S}$ can be described using a probability density with respect to the Lebesgue measure on $\mathbb{R}^{|\mathcal{S}|}$.*

Without the first assumption, two concepts $k, j \in V$ might always change together, meaning there is no data pair in which only one of them varies independently. Intuitively, this would prevent the model from disentangling them effectively. Importantly, our assumption accommodates a broad range of scenarios. E.g., it is not necessarily violated even in an extreme case where $|V| - 1$ concepts change in each pair. Moreover, it allows for the presence of statistically dependent concepts. The second criterion ensures the distribution $\mathbb{P}_{\delta_{\mathcal{S}}^c|S=s}$ does not concentrate mass on a subset of $\mathbb{R}^{|\mathcal{S}|}$ of Lebesgue measure zero. In Apx. A.4, we provide examples and illustrations of distributions that meet or fail the assumption.⁵

We are now ready to state the main identifiability result of this section. We note that its proof relies to a large extent on an existing result by Lachapelle et al. (2023).

Proposition 3 (Identifiability up to permutation). *Suppose (\hat{r}, \hat{q}) is a solution to the constrained problem of Eqns. (4) and (5) with $\beta = \mathbb{E}\|\delta_V^c\|_0$. Under Asm. 1 to 4, there exists an invertible diagonal matrix and a permutation matrix $\mathbf{D}, \mathbf{P} \in \mathbb{R}^{|\mathcal{S}| \times |\mathcal{S}|}$ such that $\hat{q} = \mathbf{A}_V \mathbf{D} \mathbf{P}$ and $\hat{r}(\mathbf{z}) = \mathbf{P}^\top \mathbf{D}^{-1} \mathbf{A}_V^\top \mathbf{z}$ for all $\mathbf{z} \in \text{Im}(\mathbf{A}_V)$, where $\text{Im}(\mathbf{A}_V)$ is the image of \mathbf{A}_V .*

Proof sketch. We outline the proof here and defer the full details to Apx. A.3. We first show that all optimal solutions of the constrained problem must reach a reconstruction loss of zero. This means that optimal solutions to the constrained problem are also optimal for the unconstrained one. Thus, these solutions must identify \mathbf{A}_V up to linear transformation, by Prop. 2. We can then rewrite the constraint as $\mathbb{E}\|\mathbf{L}^{-1} \delta_V^c\|_0 \leq \beta = \mathbb{E}\|\delta_V^c\|_0$. Here, we can reuse an

⁵See Lachapelle et al. (2023) for a strictly weaker but more technical assumption that is also sufficient for Prop. 3.

argument initially proposed by Lachapelle et al. (2023) to leverage this inequality to conclude that \mathbf{L}^{-1} must be a permutation-scaling matrix. For completeness, we present this argument in Lemma 4. It shows that, applying the matrix \mathbf{L}^{-1} to δ_V^c always strictly increases its expected sparsity, unless \mathbf{L}^{-1} is a permutation-scaling matrix. Thus, to satisfy the inequality, \mathbf{L} must be a permutation-scaling matrix.

2.5. Extracting steering vectors

In Section 2.3, we proposed using steering functions of the form $\hat{\phi}_k(\mathbf{z}) := \mathbf{z} + \hat{q}(\mathbf{e}_k)$ to perturb concepts, where \hat{q} is learned via the constrained problem of Eqns. (4) and (5). Here, we show that these steering functions are valid. Our argument relies on the identifiability guarantees presented in the previous section. Under Asm. 1 to 4, Prop. 3 shows that $\hat{q} = \mathbf{A}_V \mathbf{D} \mathbf{P}$, from which we can verify that $\hat{q}(\mathbf{e}_k) = \mathbf{D}_{\pi(k), \pi(k)} \mathbf{A} \mathbf{e}_{\pi(k)}$ for all $k \in V$, where $\pi : V \rightarrow V$ is the permutation that \mathbf{P} represents. From this, we can show that $\hat{\phi}_k$ is (almost) a steering function as per Defn. 1:

$$\begin{aligned} \hat{\phi}_k(f(g(\mathbf{c}))) &= f(g(\mathbf{c})) + \hat{q}(\mathbf{e}_k) \\ &= \mathbf{A} \mathbf{c} + \mathbf{D}_{\pi(k), \pi(k)} \mathbf{A} \mathbf{e}_{\pi(k)} \\ &= \mathbf{A}(\mathbf{c} + \mathbf{D}_{\pi(k), \pi(k)} \mathbf{e}_{\pi(k)}) \\ &= f(g(\mathbf{c} + \mathbf{D}_{\pi(k), \pi(k)} \mathbf{e}_{\pi(k)})). \end{aligned}$$

Thus, $\hat{\phi}_k$ sends the representations $\mathbf{z} = f(g(\mathbf{c}))$ to their counterfactual representations where only concept $\pi(k)$ changed. We note that, strictly speaking, this does not correspond exactly to the definition of steering function introduced in Section 2.2, since both the scale of the shift $\mathbf{D}_{\pi(k), \pi(k)}$ and the concept being manipulated $\pi(k)$ are unknown. Although the scaling and permutation indeterminacies are unavoidable with unsupervised learning, a practitioner can choose a steering vector $\hat{q}(\mathbf{e}_k)$, add different scalings of this vector to an embedding \mathbf{z} and, e.g., use it to generate the next tokens with an LLM to infer which concept the vector $\hat{q}(\mathbf{e}_k)$ affects.

Linear identifiability is insufficient. In contrast, the above strategy fails when concept shifts are only linearly identified, i.e., $\hat{q} := \mathbf{A}_V \mathbf{L}$. In this case, we see that

$$\hat{q}(\mathbf{e}_k) = \mathbf{A}_V \mathbf{L} \mathbf{e}_k = \sum_{j=1}^{|\mathcal{S}|} \mathbf{L}_{j,k} \mathbf{A} \mathbf{e}_j = \mathbf{A} \sum_{j=1}^{|\mathcal{S}|} \mathbf{L}_{j,k} \mathbf{e}_j,$$

which itself implies that

$$\begin{aligned} \hat{\phi}_k(f(g(\mathbf{c}))) &= \mathbf{A} \mathbf{c} + \mathbf{A} \sum_{j=1}^{|\mathcal{S}|} \mathbf{L}_{j,k} \mathbf{e}_j \\ &= \mathbf{A}(\mathbf{c} + \sum_{j=1}^{|\mathcal{S}|} \mathbf{L}_{j,k} \mathbf{e}_j) \\ &= f(g(\mathbf{c} + \sum_{j=1}^{|\mathcal{S}|} \mathbf{L}_{j,k} \mathbf{e}_j)). \end{aligned}$$

That is, each learned steering vector $\hat{q}(e_k)$ can potentially change every concept in V . To recover the steering vectors, we need to learn \mathbf{L}^{-1} , which requires paired samples $(\tilde{\mathbf{z}}_{j,\lambda}, \mathbf{z})$ that vary in a single concept for each concept j (Rajendran et al., 2024). This highlights the importance of enforcing sparsity, as it is the key element allowing us to go from $\hat{q} := \mathbf{A}_V \mathbf{L}$ (Prop. 2) to $\hat{q} := \mathbf{A}_V \mathbf{DP}$ (Prop. 3).

3. Empirical Studies

In this section, we investigate two main questions: (i) how well can SSAE identify concept shifts in practice, and (ii) do the steering vectors recovered by SSAE accurately steer target concepts?

Implementation details. As mentioned in Section 2.4, key to identifying steering vectors is the sparsity constraint from Eqn. (9). Two key aspects of enforcing sparsity of the learnt representation are: (i) using hard constraints rather than penalty tuning, which helps address concerns with ℓ_1 -based regularization (e.g., feature suppression (Anders et al., 2024)) and (ii) appropriate normalisation. For the former, we use the `cooper` library (Gallego-Posada & Ramirez, 2022). For the latter, we implement batch normalization (Ioffe & Szegedy, 2015) after the encoder and column normalization in the decoder at each step (Bricken et al., 2023; Gao et al., 2024). To tune the model’s hyperparameters in an unsupervised way, we use the Unsupervised Diversity Ranking (UDR) score (Duan et al., 2019), and test the model’s sensitivity on key parameters (such as the sparsity level ϵ and learning rate). For details, refer to Apx. B.

Baselines. We consider two baselines: an affine Autoencoder (`aff`), with identical architecture but no sparsity constraint, and Mean Difference (MD) vectors, which use paired observations differing in a single concept to compute $\frac{1}{n} \sum_{i=1}^n (\tilde{\mathbf{z}}_k^{(i)} - \mathbf{z}_k^{(i)}) = \frac{1}{n} \sum_{i=1}^n \lambda^{(i)} \mathbf{A} \mathbf{e}_k = \bar{\lambda} \mathbf{A} \mathbf{e}_k$ as the steering vector for concept k . We denote the concept-steered embeddings produced by each method as $\tilde{\mathbf{z}}_\eta$ (SSAE), $\tilde{\mathbf{z}}_{\text{aff}}$ (`aff`), and $\tilde{\mathbf{z}}_{\text{MD}}$ (MD).

Evaluation criteria. We measure the *degree of identifiability* via the Mean Correlation Coefficient (MCC) (Hyvarinen & Morioka, 2016; Khemakhem et al., 2020b), which computes the highest average correlation between each learned latent dimension and the true latent dimension and equals 1.0 when they are aligned perfectly up to permutation and scaling. On synthetic data, we compute MCC against known ground-truth concept representations. When ground-truth is not known, such as in experiments with

⁶This is in line with contemporary literature (Park et al., 2024; Reber et al., 2024) but is slightly misleading since the concepts are represented as binary contrasts, please refer to Apx. B.1.3 for a detailed discussion.

Table 1: Datasets comprise of paired observations $(\mathbf{x}, \tilde{\mathbf{x}})$ where \mathbf{x} and $\tilde{\mathbf{x}}$ vary in concepts $V = \{c_1, c_2, \dots, c_{|V|}\}$ across all pairs, such that for any given pair, the maximum number of varying concepts is $\max(|S|)$. *Nomenclature for semi-synthetic datasets follows the rule: identifier of the dataset indicating why we consider it, followed by $|V|$ and $\max(|S|)$: IDENTIFIER($|V|$, $\max|S|$).*

Dataset	$ V $	$\max(S)$
LANG(1, 1)	1	1
GENDER(1, 1)	1	1
BINARY(2, 2)	2	2
CORRELATED(2, 1)	2	1
CAT(135, 3) ⁶	135	3
TruthfulQA	1	1

LLMs, we compute MCC across different random initializations of the model, expecting 1.0 for models that consistently recover solutions equivalent to each other up to permutation and scaling. We use 10 decoder pairs from 5 seeds for selected model hyperparameters. Further, we evaluate whether identified representations indeed lead to higher *steering accuracy*. For this, we consider held-out single concept shift data $(\mathbf{x}, \tilde{\mathbf{x}}_k)$ and evaluate how well steering vectors learnt using multi-concept shifts steer $f(\mathbf{x})$ towards $f(\tilde{\mathbf{x}}_k)$. Then we measure the accuracy of steering by comparing $\tilde{\mathbf{z}}_k := f(\mathbf{x}) + (\mathbf{W}_d)_{\{:, \pi(k)\}}$ where and $f(\tilde{\mathbf{x}}_k)$ using cosine similarity as a measure of semantic similarity. Refer to Apx. B.1.4 for details on metrics.

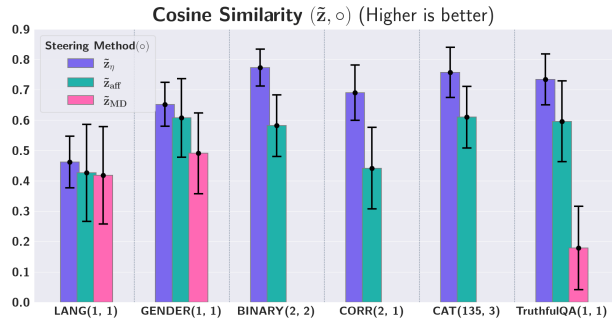


Figure 2: **A higher MCC value of the estimated decoder is associated with a greater cosine similarity.** Embeddings steered using the steering vectors from a more disentangled decoder are more similar to target embeddings, compared to embeddings steered using steering vectors from a decoder with a lower MCC value.

We focus on evaluating LLM embeddings on language datasets here. In Apx. B.4, we validate the same conclusions with experiments on synthetic data with known concepts and synthetically generated embeddings.

Experimental setup. We use text-based paired observations $(\mathbf{x}, \tilde{\mathbf{x}})$, to extract the final-layer token embedding (which is linearly identifiable following Roeder et al. (2021))

Table 2: **The mean MCC of the estimated decoder is close to 1** across all datasets considering observations ($f(\mathbf{x}), f(\tilde{\mathbf{x}})$), even for statistically dependent concepts considered in the dataset CORR(2, 1).

	SSAE	aff
LANG(1, 1)	0.9948 ± 0.0011	0.9850 ± 0.0037
GENDER(1, 1)	0.9933 ± 0.0001	0.9614 ± 0.0000
BINARY(2, 2)	0.9908 ± 0.0010	0.9356 ± 0.0001
CORR(2, 1)	0.9905 ± 0.0012	0.9283 ± 0.0772
CAT(135, 3)	0.9059 ± 0.02186	0.6607 ± 0.0189
TruthfulQA	0.9521 ± 0.0061	0.8848 ± 0.0063

Table 3: The mean MCC of the decoder of SSAE is **robust to further entanglement** across all datasets considering observations ($Lf(\mathbf{x}), Lf(\tilde{\mathbf{x}})$).

	SSAE	aff
LANG(1, 1)	0.9904 ± 0.0001	0.8765 ± 0.0068
GENDER(1, 1)	0.9912 ± 0.0001	0.8835 ± 0.0051
BINARY(2, 2)	0.9900 ± 0.0005	0.7963 ± 0.0003
CORR(2, 1)	0.9900 ± 0.0010	0.6296 ± 0.0095
CAT(135, 3)	0.9001 ± 0.0095	0.5463 ± 0.0175
TruthfulQA	0.9316 ± 0.0079	0.7511 ± 0.0115

from Llama-3.1-8B (Llama Team et al., 2024), and use the embedding of the last token as the representation, following Ma et al. (2023), to obtain representations ($f(\mathbf{x}), f(\tilde{\mathbf{x}})$).

Data. We consider both real-world language data: since existing real-world datasets used in steering research usually consist of a single concept varying across the entire dataset (Perez et al., 2022; Lin et al., 2022; Liu et al., 2024; Panickssery et al., 2024), we create a more diverse range of concept variations in semi-synthetic data. All datasets are summarised in Table 5. LANG(1, 1) (e.g., *eng* \rightarrow *french*) and GENDER(1, 1) (e.g., *masculine* \rightarrow *feminine*) vary a single concept between \mathbf{x} and $\tilde{\mathbf{x}}$. BINARY(2, 2) allows two binary concepts (language, gender) to vary jointly, and CORRELATED(2, 1) enforces correlated binary changes (e.g., *eng* \rightarrow *french* along with *eng* \rightarrow *german*). CAT(135, 3) uses shape-color-object phrases (eg: “purple toroidal shoe”) where each attribute has 10 possible values, represented via binary contrasts to produce 135 concepts in total. We apply our method to the multiple-choice track of TruthfulQA (Lin et al., 2022), creating ($\mathbf{x}, \tilde{\mathbf{x}}$) pairs by assigning \mathbf{x} to be the question paired with a wrong answer that mimics human falsehoods, and $\tilde{\mathbf{x}}$ to be a question paired with the correct answer to capture the variation of the concept truthfulness from *false* \rightarrow *true*. Details on datasets can be found in Apx. B.1.3.

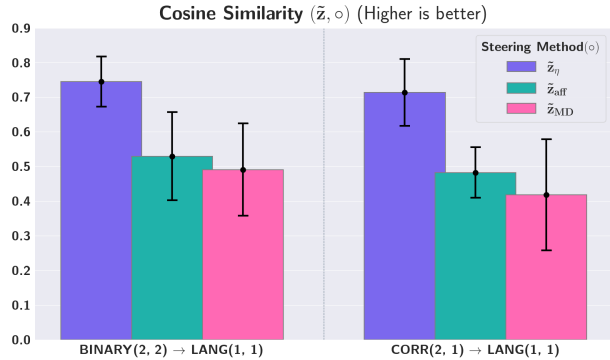


Figure 3: Embeddings steered using the proposed method show **higher OOD generalisation performance**.

How well does SSAE identify steering vectors? As shown in Table 2, SSAE achieves consistently high MCC values, empirically corroborating Prop. 3. On simpler datasets such as LANG(1, 1) and GENDER(1, 1), SSAE and the affine (aff) baseline perform comparably, suggesting that these concepts are relatively easy to decode from the LLM’s final layer, as compared to the concept of truthfulness (in the case of TruthfulQA). Further, when the number of concepts or the correlation between them increases (e.g., CORR(2, 1) and especially CAT(135, 3)), SSAE shows a clearer advantage. In contrast, the aff baseline’s MCC scores either sharply decline or exhibit high variance (as in the case of CORR(2, 1)). We interpret these findings as evidence that simpler datasets do not fully stress-test identifiability. Consequently, we present robustness experiments—further entangling the embeddings and deliberately misspecifying the model (see Apx. B.3)—to determine whether SSAE exhibits benefits under more demanding conditions.

How robust is SSAE to increased entanglement? Table 3 demonstrates that, once we apply a dense linear invertible transformation \mathbf{L} to the embeddings to generate ($Lf(\mathbf{x}), Lf(\tilde{\mathbf{x}})$), the gap between SSAE and the affine baseline widens. This larger gap indicates that further entangling the difference vectors makes it more challenging for the baseline to identify meaningful steering directions, whereas SSAE remains robust. The worsening performance of aff after the entanglement is applied suggests that LLM representations might already somewhat disentangle some concepts or encode them through sparse or simple transformations, an idea that requires deeper investigation. Although SSAE generally outperforms aff across several datasets, drawing conclusions based solely on MCC might be premature, especially when considering their ultimate deployment to the problem of steering, which we evaluate next.

Does identifiable steering translate to better steering? Figure 2 illustrates how identifying steering vectors benefits

the downstream task of steering embeddings, while Figure 3 shows that the identified steering vectors also transfer effectively to out-of-distribution datasets—provided that the concept in question is present. Specifically, for the experiments in Figure 2, we consider a held-out test set of pairs $(\mathbf{x}, \tilde{\mathbf{x}}_k) \forall k \in V$, each varying by a single concept, and compare the cosine similarity between the steered embeddings and target embeddings. By design, the dataset LANG(1, 1) consists of examples of a language change from *eng* \rightarrow *french* for words stemming from another general concept, *household objects*, while the samples in BINARY(2, 2) which have the same language change correspond to samples of *professions*. Similarly, the dataset CORR(2, 1) consists of *eng* \rightarrow *french* and *eng* \rightarrow *german* changes corresponding to words describing *professions*. Please refer to Apx. B.1.3 for details. The hypothesis here is that the steering vector for *eng* \rightarrow *french* from an identifiable model should be able to generalise between datasets with samples varying along concepts in the same subset $S \subseteq V$ but for which the set of non-varying concepts \bar{V} varies. Figure 2 also reveals that even slight differences in MCC can translate into pronounced variations in both in-distribution and OOD steering accuracy, indicating that solely evaluating identifiable representation learning methods on MCC is not sufficient.

4. Related work

Linear representation hypothesis. This paper builds on the linear representation hypothesis that language models encode concepts linearly. Several papers provide empirical evidence for this hypothesis (Mikolov et al., 2013; Gittens et al., 2017; Ethayarajh et al., 2019; Allen & Hospedales, 2019; Seonwoo et al., 2019; Burns et al., 2024; Li et al., 2024a; Moschella et al., 2023; Tigges et al., 2023; Nanda et al., 2023; Nissim et al., 2020; Ravfogel et al., 2020a; Park et al., 2023). Recent work also provides theoretical justification for why linear properties might consistently emerge across models that perform next-token prediction (Roeder et al., 2021; Jiang et al., 2024; Marconato et al., 2024; Park et al., 2024).

Interpretability of LLMs. This paper contributes to the literature on interpretability and steering of LLMs. Much of the work on finding concepts in LLM representations for steering relies on supervision, either from paired observations with a single-concept shift (Panickssery et al., 2024; Turner et al., 2024; Rimsky et al., 2024; Li et al., 2024a) or from examples of target LLM completions to prompts (Subramani et al., 2022). This prior work also focuses on applying the same steering vector to all examples, implicitly relying on the linear representation hypothesis as justification. In contrast, we make the assumption precise, and show how it leads to steering vectors. This paper also departs from supervised learning and focuses on learning with limited

supervision. In this way, we propose a method that is similar to sparse autoencoders (SAEs) (Templeton et al., 2024; Engels et al., 2024; Cunningham et al., 2023; Rajamanoharan et al., 2024; Gao et al., 2024). In contrast, our proposed method fits concept shifts, and provably identifies steering vectors while SAEs do not enjoy identifiability guarantees.

Causal representation learning. Finally, this paper builds on causal representation learning results that leverage sparsity constraints. Ahuja et al. (2022), Locatello et al. (2020a), and Brehmer et al. (2022) consider sparse latent perturbations and paired observations. In contrast, we focus on learning from multi-concept shifts. Lachapelle et al. (2022) focus on sparse interventions and sparse transitions in temporal settings, while Lachapelle et al. (2023), Layne et al. (2024), Xu et al. (2024), and Fumero et al. (2023) leverage sparse dependencies between latents and tasks. In this paper, we adapt these assumptions and technical results for a novel setting: discovering steering vectors from LLM representations based on concept shift data. Although they do not leverage a sparsity constraint, the setting in Rajendran et al. (2024) is the most similar to ours, aiming to recover linear subspaces that capture concepts from observations generated by a nonlinear mixing function. They leverage concept-conditional datasets to prove that these concept subspaces are identified up to linear transformations. In contrast, we focus on concept shifts, and propose a regularized objective that recovers them up to permutation and scaling, allowing for straightforward steering vector discovery.

5. Conclusion

We propose Sparse Shift Autoencoders (SSAEs) for discovering accurate steering vectors from multi-concept paired observations as an alternative to both SAEs and approaches relying on supervised data. Key to this result are the identifiability guarantees that the SSAE enjoys as a consequence of considering sparse concept shifts. We study the SSAE empirically, using Llama3.1 embeddings on several real language tasks, and find evidence that the method facilitates accurate steering learned via limited supervision. However, we stress that these experiments are intended to validate the identifiability results in Section 2 and their implications for accurate steering. Although we include real-world data (TruthfulQA), to fully understand the impacts of the SSAE on steering research, especially LLM alignment, more evaluation is needed on embeddings from more complex datasets, on more challenging tasks (e.g., MTEB (Muennighoff et al., 2023)), and by generating text with steered embeddings to assess model behavior. Rigorous large-scale evaluations are a promising avenue for future work. Such evaluations would benefit from more expansive real-world benchmarks and a more nuanced approach to categorical concepts—one that moves beyond reducing them to binary contrasts.

Acknowledgements

We thank Devon Hjelm, Nino Scherrer, Arkil Patel, Sahil Verma, Arihant Jain, and Divyat Mahajan for helpful discussions. DS acknowledges support from NSERC Discovery Grant RGPIN-2023-04869, and a Canada-CIFAR AI Chair.

Impact Statement

This paper presents technical advancements to a new field of machine learning focused on steering the behaviour of large language models at inference time, i.e., without requiring access to the model’s parameters. Steering methods have already begun to play a role in the alignment of LLMs to be e.g., more truthful. We present a new method that could speed up steering research by allowing practitioners to recover steering vectors without the need for supervision, a previous limitation of steering methods. As such, this work could have a positive impact on LLM safety and alignment research. Nevertheless, we flag that contributions towards steering such as ours should be empirically evaluated carefully to avoid over-claiming LLM safety. We acknowledge that while the empirical studies we conduct demonstrate the advantages of identifiable methods such as SSAFE for steering, further evaluation is necessary to the method’s use in AI safety research.

References

- Ahuja, K., Hartford, J. S., and Bengio, Y. Weakly supervised representation learning with sparse perturbations. *Advances in Neural Information Processing Systems*, 35: 15516–15528, 2022. Cited on pages 4, 8, and 20.
- Allen, C. and Hospedales, T. Analogies explained: Towards understanding word embeddings, 2019. URL <https://arxiv.org/abs/1901.09813>. Cited on page 8.
- Anders, E., Neo, C., Hoelscher-Obermaier, J., and Howard, J. N. Sparse autoencoders find composed features in small toy models. <https://www.lesswrong.com/posts/a5wwqza2cY3W7L9cj/sparse-autoencoders-find-composed-features-in-small-toy>, 2024. Cited on pages 6 and 26.
- Brehmer, J., de Haan, P., Lippe, P., and Cohen, T. Weakly supervised causal representation learning, 2022. URL <https://arxiv.org/abs/2203.16437>. Cited on page 8.
- Bricken, T., Templeton, A., Batson, J., Chen, B., Jermyn, A., Conerly, T., Turner, N., Anil, C., Denison, C., Askell, A., Lasenby, R., Wu, Y., Kravec, S., Schiefer, N., Maxwell, T., Joseph, N., Hatfield-Dodds, Z., Tamkin, A., Nguyen, K., McLean, B., Burke, J. E., Hume, T., Carter, S., Henighan, T., and Olah, C. Towards monosemanticity: Decomposing language models with dictionary learning. *Transformer Circuits Thread*, 2023. URL <https://transformer-circuits.pub/2023/monosemantic-features/index.html>. Cited on pages 1, 4, 6, and 21.
- Burns, C., Ye, H., Klein, D., and Steinhardt, J. Discovering latent knowledge in language models without supervision, 2024. URL <https://arxiv.org/abs/2212.03827>. Cited on page 8.
- Cunningham, H., Ewart, A., Riggs, L., Huben, R., and Sharkey, L. Sparse autoencoders find highly interpretable features in language models, 2023. URL <https://arxiv.org/abs/2309.08600>. Cited on pages 1, 2, and 8.
- Duan, S., Matthey, L., Saraiva, A., Watters, N., Burgess, C. P., Lerchner, A., and Higgins, I. Unsupervised model selection for variational disentangled representation learning. *arXiv preprint arXiv:1905.12614*, 2019. Cited on pages 6 and 22.
- Elhage, N., Hume, T., Olsson, C., Schiefer, N., Henighan, T., Kravec, S., Hatfield-Dodds, Z., Lasenby, R., Drain, D., Chen, C., Grosse, R., McCandlish, S., Kaplan, J., Amodei, D., Wattenberg, M., and Olah, C. Toy models of superposition. *Transformer Circuits Thread*, 2022. URL https://transformer-circuits.pub/2022/toy_model/index.html. Cited on page 2.
- Engels, J., Liao, I., Michaud, E. J., Gurnee, W., and Tegmark, M. Not all language model features are linear, 2024. URL <https://arxiv.org/abs/2405.14860>. Cited on page 8.
- Ethayarajh, K., Duvenaud, D., and Hirst, G. Towards understanding linear word analogies, 2019. URL <https://arxiv.org/abs/1810.04882>. Cited on page 8.
- Fumero, M., Wenzel, F., Zancato, L., Achille, A., Rodolà, E., Soatto, S., Schölkopf, B., and Locatello, F. Leveraging sparse and shared feature activations for disentangled representation learning, 2023. URL <https://arxiv.org/abs/2304.07939>. Cited on page 8.
- Gallego-Posada, J. and Ramirez, J. Cooper: a toolkit for Lagrangian-based constrained optimization. <https://github.com/cooper-org/cooper>, 2022. Cited on pages 4, 6, and 22.
- Gao, L., la Tour, T. D., Tillman, H., Goh, G., Troll, R., Radford, A., Sutskever, I., Leike, J., and Wu, J. Scaling and evaluating sparse autoencoders. *arXiv preprint arXiv:2406.04093*, 2024. Cited on pages 4, 6, 8, and 21.

- Gidel, G., Berard, H., Vignoud, G., Vincent, P., and Lacoste-Julien, S. A variational inequality perspective on generative adversarial networks, 2020. URL <https://arxiv.org/abs/1802.10551>. Cited on pages 4 and 22.
- Gittens, A., Achlioptas, D., and Mahoney, M. W. Skipgram - Zipf + uniform = vector additivity. In Barzilay, R. and Kan, M.-Y. (eds.), *Proceedings of the 55th Annual Meeting of the Association for Computational Linguistics (Volume 1: Long Papers)*, pp. 69–76, Vancouver, Canada, July 2017. Association for Computational Linguistics. doi: 10.18653/v1/P17-1007. URL <https://aclanthology.org/P17-1007>. Cited on page 8.
- Hinton, G. E. et al. Learning distributed representations of concepts. In *Proceedings of the eighth annual conference of the cognitive science society*, volume 1, pp. 12. Amherst, MA, 1986. Cited on page 4.
- Hyvarinen, A. and Morioka, H. Unsupervised feature extraction by time-contrastive learning and nonlinear ica, 2016. URL <https://arxiv.org/abs/1605.06336>. Cited on pages 6 and 23.
- Ioffe, S. and Szegedy, C. Batch normalization: Accelerating deep network training by reducing internal covariate shift, 2015. URL <https://arxiv.org/abs/1502.03167>. Cited on page 6.
- Jiang, Y., Rajendran, G., Ravikumar, P., Aragam, B., and Veitch, V. On the origins of linear representations in large language models, 2024. URL <https://arxiv.org/abs/2403.03867>. Cited on pages 2, 4, 8, and 26.
- Khemakhem, I., Kingma, D., Monti, R., and Hyvärinen, A. Variational autoencoders and nonlinear ica: A unifying framework. In *Proceedings of the Twenty Third International Conference on Artificial Intelligence and Statistics*, 2020a. Cited on page 4.
- Khemakhem, I., Monti, R. P., Kingma, D. P., and Hyvärinen, A. Ice-beem: Identifiable conditional energy-based deep models based on nonlinear ica, 2020b. URL <https://arxiv.org/abs/2002.11537>. Cited on pages 6, 23, and 25.
- Korpelevich, G. M. The extragradient method for finding saddle points and other problems. *Matecon*, 12:747–756, 1976. Cited on page 22.
- Lachapelle, S., Rodriguez, P., Sharma, Y., Everett, K. E., Le Priol, R., Lacoste, A., and Lacoste-Julien, S. Disentanglement via mechanism sparsity regularization: A new principle for nonlinear ica. In *Conference on Causal Learning and Reasoning*, pp. 428–484. PMLR, 2022. Cited on page 8.
- Lachapelle, S., Deleu, T., Mahajan, D., Mitliagkas, I., Bengio, Y., Lacoste-Julien, S., and Bertrand, Q. Synergies between disentanglement and sparsity: Generalization and identifiability in multi-task learning. In *International Conference on Machine Learning*, 2023. Cited on pages 2, 5, 8, 16, 17, 18, 19, and 26.
- Layne, E., Hartford, J., Lachapelle, S., Blanchette, M., and Sridhar, D. Sparsity regularization via tree-structured environments for disentangled representations, 2024. URL <https://arxiv.org/abs/2405.20482>. Cited on page 8.
- Li, K., Patel, O., Viégas, F., Pfister, H., and Wattenberg, M. Inference-time intervention: Eliciting truthful answers from a language model, 2024a. URL <https://arxiv.org/abs/2306.03341>. Cited on page 8.
- Li, N., Pan, A., Gopal, A., Yue, S., Berrios, D., Gatti, A., Li, J. D., Dombrowski, A.-K., Goel, S., Phan, L., Mukobi, G., Helm-Burger, N., Lababidi, R., Justen, L., Liu, A. B., Chen, M., Barrass, I., Zhang, O., Zhu, X., Tamirisa, R., Bharathi, B., Khoja, A., Zhao, Z., Herbert-Voss, A., Breuer, C. B., Marks, S., Patel, O., Zou, A., Mazeika, M., Wang, Z., Oswal, P., Lin, W., Hunt, A. A., Tienken-Harder, J., Shih, K. Y., Talley, K., Guan, J., Kaplan, R., Steneker, I., Campbell, D., Jokubaitis, B., Levinson, A., Wang, J., Qian, W., Karmakar, K. K., Basart, S., Fitz, S., Levine, M., Kumaraguru, P., Tupakula, U., Varadharajan, V., Wang, R., Shoshitaishvili, Y., Ba, J., Esvelt, K. M., Wang, A., and Hendrycks, D. The wmdp benchmark: Measuring and reducing malicious use with unlearning, 2024b. URL <https://arxiv.org/abs/2403.03218>. Cited on page 1.
- Lin, S., Hilton, J., and Evans, O. Truthfulqa: Measuring how models mimic human falsehoods, 2022. URL <https://arxiv.org/abs/2109.07958>. Cited on pages 7 and 23.
- Liu, S., Ye, H., Xing, L., and Zou, J. In-context vectors: Making in context learning more effective and controllable through latent space steering, 2024. URL <https://arxiv.org/abs/2311.06668>. Cited on page 7.
- Llama Team et al. The llama 3 herd of models, 2024. URL <https://arxiv.org/abs/2407.21783>. Cited on pages 1, 7, and 26.
- Locatello, F., Bauer, S., Lucic, M., Rätsch, G., Gelly, S., Schölkopf, B., and Bachem, O. Challenging common assumptions in the unsupervised learning of disentangled representations, 2019. URL <https://arxiv.org/abs/1811.12359>. Cited on page 22.

- Locatello, F., Poole, B., Rätsch, G., Schölkopf, B., Bachem, O., and Tschannen, M. Weakly-supervised disentanglement without compromises. In *International conference on machine learning*, pp. 6348–6359. PMLR, 2020a. Cited on page 8.
- Locatello, F., Poole, B., Rätsch, G., Schölkopf, B., Bachem, O., and Tschannen, M. Weakly-supervised disentanglement without compromises, 2020b. Cited on page 3.
- Lopez-Paz, D., Hennig, P., and Schölkopf, B. The randomized dependence coefficient. *Advances in neural information processing systems*, 26, 2013. Cited on page 25.
- Ma, X., Wang, L., Yang, N., Wei, F., and Lin, J. Fine-tuning llama for multi-stage text retrieval, 2023. URL <https://arxiv.org/abs/2310.08319>. Cited on page 7.
- Mairal, J., Bach, F., Ponce, J., and Sapiro, G. Online dictionary learning for sparse coding. In *Proceedings of the 26th annual international conference on machine learning*, pp. 689–696, 2009. Cited on page 2.
- Marconato, E., Lachapelle, S., Weichwald, S., and Gresele, L. All or none: Identifiable linear properties of next-token predictors in language modeling. *arXiv preprint arXiv:2410.23501*, 2024. Cited on pages 4 and 8.
- Mikolov, T., Yih, W.-t., and Zweig, G. Linguistic regularities in continuous space word representations. In Vanderwende, L., Daumé III, H., and Kirchhoff, K. (eds.), *Proceedings of the 2013 Conference of the North American Chapter of the Association for Computational Linguistics: Human Language Technologies*, pp. 746–751, Atlanta, Georgia, June 2013. Association for Computational Linguistics. URL <https://aclanthology.org/N13-1090>. Cited on pages 2, 4, and 8.
- Moschella, L., Maiorca, V., Fumero, M., Norelli, A., Locatello, F., and Rodolà, E. Relative representations enable zero-shot latent space communication, 2023. URL <https://arxiv.org/abs/2209.15430>. Cited on page 8.
- Muennighoff, N., Tazi, N., Magne, L., and Reimers, N. Mteb: Massive text embedding benchmark, 2023. URL <https://arxiv.org/abs/2210.07316>. Cited on page 8.
- Nanda, N., Lee, A., and Wattenberg, M. Emergent linear representations in world models of self-supervised sequence models, 2023. URL <https://arxiv.org/abs/2309.00941>. Cited on page 8.
- Nissim, M., van Noord, R., and van der Goot, R. Fair is better than sensational: Man is to doctor as woman is to doctor. *Computational Linguistics*, 46(2):487–497, June 2020. doi: 10.1162/coli_a.00379. URL <https://aclanthology.org/2020.cl-2.7>. Cited on page 8.
- Panickssery, N., Gabrieli, N., Schulz, J., Tong, M., Hubinger, E., and Turner, A. M. Steering llama 2 via contrastive activation addition, 2024. URL <https://arxiv.org/abs/2312.06681>. Cited on pages 7 and 8.
- Park, K., Choe, Y. J., and Veitch, V. The linear representation hypothesis and the geometry of large language models, 2023. Cited on pages 8 and 26.
- Park, K., Choe, Y. J., Jiang, Y., and Veitch, V. The geometry of categorical and hierarchical concepts in large language models, 2024. URL <https://arxiv.org/abs/2406.01506>. Cited on pages 6 and 8.
- Perez, E., Ringer, S., Lukošiuūtė, K., Nguyen, K., Chen, E., Heiner, S., Pettit, C., Olsson, C., Kundu, S., Kavavath, S., Jones, A., Chen, A., Mann, B., Israel, B., Seethor, B., McKinnon, C., Olah, C., Yan, D., Amodei, D., Amodei, D., Drain, D., Li, D., Tran-Johnson, E., Khundadze, G., Kernion, J., Landis, J., Kerr, J., Mueller, J., Hyun, J., Landau, J., Ndousse, K., Goldberg, L., Lovitt, L., Lucas, M., Sellitto, M., Zhang, M., Kingsland, N., Elhage, N., Joseph, N., Mercado, N., Das-Sarma, N., Rausch, O., Larson, R., McCandlish, S., Johnston, S., Kravec, S., Showk, S. E., Lanham, T., Telleen-Lawton, T., Brown, T., Henighan, T., Hume, T., Bai, Y., Hatfield-Dodds, Z., Clark, J., Bowman, S. R., Askell, A., Grosse, R., Hernandez, D., Ganguli, D., Hubinger, E., Schiefer, N., and Kaplan, J. Discovering language model behaviors with model-written evaluations, 2022. URL <https://arxiv.org/abs/2212.09251>. Cited on page 7.
- Rahn, N., D’Oro, P., and Bellemare, M. G. Controlling large language model agents with entropic activation steering, 2024. URL <https://arxiv.org/abs/2406.00244>. Cited on page 1.
- Rajamanoharan, S., Conmy, A., Smith, L., Lieberum, T., Varma, V., Kramár, J., Shah, R., and Nanda, N. Improving dictionary learning with gated sparse autoencoders, 2024. URL <https://arxiv.org/abs/2404.16014>. Cited on page 8.
- Rajendran, G., Buchholz, S., Aragam, B., Schölkopf, B., and Ravikumar, P. Learning interpretable concepts: Unifying causal representation learning and foundation models, 2024. Cited on pages 2, 4, 6, and 8.
- Ravfogel, S., Elazar, Y., Gonen, H., Twiton, M., and Goldberg, Y. Null it out: Guarding protected attributes by iterative nullspace projection. In Jurafsky, D., Chai, J., Schluter, N., and Tetreault, J. (eds.), *Proceedings of*

- the 58th Annual Meeting of the Association for Computational Linguistics, pp. 7237–7256, Online, July 2020a. Association for Computational Linguistics. doi: 10.18653/v1/2020.acl-main.647. URL <https://aclanthology.org/2020.acl-main.647>. Cited on page 8.
- Ravfogel, S., Elazar, Y., Gonen, H., Twiton, M., and Goldberg, Y. Null it out: Guarding protected attributes by iterative nullspace projection. *arXiv preprint arXiv:2004.07667*, 2020b. Cited on page 4.
- Reber, D., Richardson, S., Nief, T., Garbacea, C., and Veitch, V. Rate: Score reward models with imperfect rewrites of rewrites. *arXiv preprint arXiv:2410.11348*, 2024. Cited on page 6.
- Rimsky, N., Gabrieli, N., Schulz, J., Tong, M., Hubinger, E., and Turner, A. M. Steering llama 2 via contrastive activation addition, 2024. Cited on pages 1, 3, and 8.
- Roeder, G., Metz, L., and Kingma, D. On linear identifiability of learned representations. In *International Conference on Machine Learning*, pp. 9030–9039. PMLR, 2021. Cited on pages 4, 6, and 8.
- Rumelhart, D. E. and Abrahamson, A. A. A model for analogical reasoning. *Cognitive Psychology*, 5(1):1–28, 1973. Cited on page 4.
- Seonwoo, Y., Park, S., Kim, D., and Oh, A. Additive compositionality of word vectors. In Xu, W., Ritter, A., Baldwin, T., and Rahimi, A. (eds.), *Proceedings of the 5th Workshop on Noisy User-generated Text (W-NUT 2019)*, pp. 387–396, Hong Kong, China, November 2019. Association for Computational Linguistics. doi: 10.18653/v1/D19-5551. URL <https://aclanthology.org/D19-5551>. Cited on page 8.
- Shen, T., Lei, T., Barzilay, R., and Jaakkola, T. Style transfer from non-parallel text by cross-alignment, 2017. URL <https://arxiv.org/abs/1705.09655>. Cited on page 3.
- Stephane, M. A wavelet tour of signal processing, 1999. Cited on page 2.
- Subramani, N., Suresh, N., and Peters, M. E. Extracting latent steering vectors from pretrained language models. *ACL Findings*, 2022. Cited on pages 1 and 8.
- Templeton, A., Conerly, T., Marcus, J., Lindsey, J., Bricken, T., Chen, B., Pearce, A., Citro, C., Ameisen, E., Jones, A., Cunningham, H., Turner, N. L., McDougall, C., MacDiarmid, M., Freeman, C. D., Sumers, T. R., Rees, E., Batson, J., Jermyn, A., Carter, S., Olah, C., and Henighan, T. Scaling monosemanticity: Extracting interpretable features from claude 3 sonnet. *Transformer Circuits Thread*, 2024. URL <https://transformer-circuits.pub/2024/scaling-monosemanticity/index.html>. Cited on pages 2, 8, and 21.
- Tigges, C., Hollinsworth, O. J., Geiger, A., and Nanda, N. Linear representations of sentiment in large language models, 2023. URL <https://arxiv.org/abs/2310.15154>. Cited on page 8.
- Turner, A. M., Thiergart, L., Leech, G., Udell, D., Vazquez, J. J., Mini, U., and MacDiarmid, M. Steering language models with activation engineering, 2024. URL <https://arxiv.org/abs/2308.10248>. Cited on pages 1, 3, and 8.
- Xu, D., Yao, D., Lachapelle, S., Taslakian, P., von Kügelgen, J., Locatello, F., and Magliacane, S. A sparsity principle for partially observable causal representation learning. In *Proceedings of the 41st International Conference on Machine Learning*, 2024. Cited on pages 2, 4, 5, 8, 16, 17, and 26.

..we understand the world by studying change, not by studying things..

As quoted in the Order of Time, Anaximander

Contents

1	Introduction	1
2	Identifiable learning of steering vectors	2
2.1	Preliminaries	2
2.2	Problem formulation	2
2.3	Learning steering vectors via multi-concept shifts	3
2.4	Identifiability analysis	4
2.5	Extracting steering vectors	5
3	Empirical Studies	6
4	Related work	8
5	Conclusion	8
A	Theory	14
A.1	Notation and Glossary	14
A.2	Proof of Prop. 2 (linear identifiability)	15
A.3	Proof of Prop. 3 (permutation identifiability)	16
A.4	Distributions satisfying Asm. 4	19
A.5	Interpreting the Linear Representation Hypothesis	19
B	Implementation and experimental details	21
B.1	SSAE Architecture	21
B.1.1	Model Selection via Unsupervised Diversity Ranking (UDR)	22
B.1.2	Sparse optimization	23
B.1.3	Datasets	23
B.1.4	Mean Correlation Coefficient: Gateway to Interpreting Latent Dimensions	23
B.2	Cosine Similarity	25
B.3	2 nd Test of robustness: impact of increasing the dimensionality of the encoder’s output	26
B.4	Synthetic Experiments	26

A. Theory

A.1. Notation and Glossary

General notation

k	integer
$[k]$	set of all integers between 1 and k , inclusively
$S \subseteq [k]$	set
$ S $	cardinality of a set
$S \setminus S'$	set subtraction (set of elements of S that are not in S')
λ	scalar
\mathbf{x}	vector and vector-valued random variables
x_k	element k of a random vector \mathbf{x}
\mathbf{x}_S	subvector with element x_i for $i \in S$
\mathbf{A}	matrix
$\mathbf{A}_{i,j}$	element i, j of matrix \mathbf{A}
$\mathbf{A}_{:,i}$	column i of matrix \mathbf{A}
\mathbf{A}_S	matrix with columns $\mathbf{A}_{:,j}$ for $j \in S$
\mathbf{A}^+	pseudo-inverse of a matrix \mathbf{A}
$\mathbf{e}_k \in \mathbb{R}^n$	standard basis vector of the form $[0, \dots, 0, 1, 0, \dots, 0]$ with a 1 at position k
$f : \mathcal{X} \rightarrow \mathcal{Z}$	function f with domain \mathcal{X} and codomain \mathcal{Z}
$f \circ g$	composition of the functions f and g
$\ \mathbf{x}\ _p$	ℓ_p norm of \mathbf{x}
$\frac{\partial y}{\partial x}$	partial derivative of y with respect to x
$\nabla_{\mathbf{x}} f(\mathbf{x}) \in \mathbb{R}^{m \times n}$	Jacobian matrix of $f : \mathbb{R}^n \rightarrow \mathbb{R}^m$
$\nabla_{\mathbf{x}}^2 f(\mathbf{x}) \in \mathbb{R}^{n \times n}$	Hessian matrix of $f : \mathbb{R}^n \rightarrow \mathbb{R}$
\mathbb{P}	probability measure/distribution
$\mathbb{E}_{\mathbf{x}}[f(\mathbf{x})]$	expectation of $f(\mathbf{x})$ with respect to \mathbf{x}

Glossary

$\mathbf{x} \in \mathbb{R}^{d_x}$	observation
$\mathbf{z} \in \mathbb{R}^{d_z}$	pretrained representation
$\mathbf{c} \in \mathbb{R}^{d_c}$	ground-truth concept vector
$\tilde{\mathbf{c}}_{k,\lambda}$	ground-truth concept vector after varying concept k by λ from \mathbf{c}
$\tilde{\mathbf{x}}_{k,\lambda}$	observation corresponding to $\tilde{\mathbf{c}}_{k,\lambda}$
$\tilde{\mathbf{z}}_{k,\lambda}$	pretrained representation corresponding to $\tilde{\mathbf{c}}_{k,\lambda}$
$\mathcal{X} \subseteq \mathbb{R}^{d_x}$	support of observations
$\mathcal{Z} \subseteq \mathbb{R}^{d_z}$	support of pretrained representations
$\mathcal{C} \subseteq \mathbb{R}^{d_c}$	support of ground-truth concept vectors
$S \subseteq [d_c]$	subset of varying concepts in a given pair $(\mathbf{x}, \tilde{\mathbf{x}})$
$V \subseteq [d_c]$	subset of concepts allowed to vary between \mathbf{x} and $\tilde{\mathbf{x}}$
$\boldsymbol{\delta}^c$	concept shift vector
$\hat{\boldsymbol{\delta}}^c$	estimated concept shift vector
$\boldsymbol{\delta}^z$	pretrained representation shift vector
$g : \mathcal{C} \rightarrow \mathcal{X}$	map from concept representations to observations
$f : \mathcal{X} \rightarrow \mathcal{Z}$	map from observations to learned representations
$r : \mathcal{Z} \rightarrow \mathcal{C}$	encoding function
$\hat{r} : \mathcal{C} \rightarrow \mathcal{Z}$	estimated encoding function
$q : \mathcal{C} \rightarrow \mathcal{Z}$	decoding function
$\hat{q} : \mathcal{C} \rightarrow \mathcal{Z}$	estimated decoding function
$\phi_{k,\lambda} : \mathcal{Z} \rightarrow \mathcal{Z}$	steering function
$\hat{\phi}_{k,\lambda} : \mathcal{Z} \rightarrow \mathcal{Z}$	estimated steering function
\mathbf{A}	linear map between concept representations and learnt representations

A.2. Proof of Prop. 2 (linear identifiability)

Proposition 2 (Linear identifiability). *Suppose (\hat{r}, \hat{q}) is a solution to the unconstrained problem of Eqn. (4). Under Asm. 1 to 3, there exists an invertible matrix $\mathbf{L} \in \mathbb{R}^{|V| \times |V|}$ such that $\hat{q} = \mathbf{A}_V \mathbf{L}$ and $\hat{r}(\mathbf{z}) = \mathbf{L}^{-1} \mathbf{A}_V^\dagger \mathbf{z}$ for all $\mathbf{z} \in \text{Im}(\mathbf{A}_V)$, where $\text{Im}(\mathbf{A}_V)$ is the image of \mathbf{A}_V .*⁷

Proof. We note that the solution $q^* := \mathbf{A}_V$ and $r^* := \mathbf{A}_V^\dagger$ minimizes the loss since

$$\mathbb{E}_{\mathbf{x}, \tilde{\mathbf{x}}} \|\boldsymbol{\delta}^z - q^*(r^*(\boldsymbol{\delta}^z))\|_2^2 = \mathbb{E}_{\mathbf{x}, \tilde{\mathbf{x}}} \|\boldsymbol{\delta}^z - \mathbf{A}_V \mathbf{A}_V^\dagger \boldsymbol{\delta}^z\|_2^2 \quad (13)$$

$$= \mathbb{E}_{\mathbf{c}, \tilde{\mathbf{c}}} \|\mathbf{A}_V \boldsymbol{\delta}_V^c - \mathbf{A}_V (\mathbf{A}_V^\dagger \mathbf{A}_V) \boldsymbol{\delta}_V^c\|_2^2 \quad (14)$$

$$= \mathbb{E}_{\mathbf{c}, \tilde{\mathbf{c}}} \|\mathbf{A}_V \boldsymbol{\delta}_V^c - \mathbf{A}_V \boldsymbol{\delta}_V^c\|_2^2 \quad (15)$$

$$= 0, \quad (16)$$

⁷We might not have $\hat{r}(\mathbf{z}) = \mathbf{L} \mathbf{A}_V^\dagger \mathbf{z}$ for $\mathbf{z} \notin \text{Im}(\mathbf{A}_V)$, since the behavior of \hat{r} is unconstrained by the objective outside the support of $\boldsymbol{\delta}^z$, i.e., outside $\text{Im}(\mathbf{A}_V)$.

where we used the fact that \mathbf{A}_V is injective and thus $\mathbf{A}_V^+ \mathbf{A}_V = \mathbf{I}$. This means all optimal solutions must reach zero loss.

Now consider an arbitrary minimizer (\hat{r}, \hat{q}) . Since it is a minimizer, it must reach zero loss, i.e.

$$\mathbb{E}_{\mathbf{x}, \bar{\mathbf{x}}} \|\delta^z - \hat{q}(\hat{r}(\delta^z))\|_2^2 = 0 \quad (17)$$

$$\mathbb{E}_{\mathbf{c}, \bar{\mathbf{c}}} \|\mathbf{A}_V \delta_V^c - \hat{q}(\hat{r}(\mathbf{A}_V \delta_V^c))\|_2^2 = 0 \quad (18)$$

This means we must have

$$\mathbf{A}_V \delta_V^c = \hat{q}(\hat{r}(\mathbf{A}_V \delta_V^c)), \text{ almost everywhere w.r.t. } p(\delta_V^c). \quad (19)$$

Because all functions both on the left and the right hand side are continuous, the equality must hold on the support of $p(\delta_V^c)$, which we denote by Δ_V^c . Moreover, since \hat{r} and \hat{q} are linear, they can be represented as matrices, namely $\mathbf{R} \in \mathbb{R}^{|V| \times d_z}$ and $\mathbf{Q} \in \mathbb{R}^{d_z \times |V|}$. We can thus rewrite Eqn. (19) as

$$\mathbf{A}_V \delta_V^c = \mathbf{Q} \mathbf{R} \mathbf{A}_V \delta_V^c, \quad (20)$$

which holds for all $\delta_V^c \in \Delta_V^c$. By Asm. 3, we know there exists a set of $|V|$ linearly independent vectors in Δ_V^c . Construct a matrix $\mathbf{C} \in \mathbb{R}^{|V| \times |V|}$ whose columns are these linearly independent vectors. Note that \mathbf{C} is invertible, by construction.

Since this Eqn. (20) holds for all $\delta_V^c \in \Delta_V^c$, we can write

$$\mathbf{A}_V \mathbf{C} = \mathbf{Q} \mathbf{R} \mathbf{A}_V \mathbf{C} \quad (21)$$

$$\mathbf{A}_V = \mathbf{Q} \mathbf{R} \mathbf{A}_V, \quad (22)$$

where we right-multiplied by \mathbf{C}^{-1} on both sides. Since \mathbf{A}_V is injective (Asm. 2), we must have that $\mathbf{R} \mathbf{A}_V$ is injective as well. But since $\mathbf{R} \mathbf{A}_V$ is a square matrix, injectivity implies invertibility. Let us define $\mathbf{L} := (\mathbf{R} \mathbf{A}_V)^{-1}$. We thus have

$$\mathbf{A}_V = \mathbf{Q} \mathbf{L}^{-1} \quad (23)$$

$$\hat{q} = \mathbf{Q} = \mathbf{A}_V \mathbf{L}, \quad (24)$$

which proves the first part of the statement.

Now, we show that, for all $\mathbf{z} \in \text{Im}(\mathbf{A}_V)$, $\mathbf{R} \mathbf{z} = \mathbf{L} \mathbf{A}_V^+ \mathbf{z}$. Take some $\mathbf{z} \in \text{Im}(\mathbf{A}_V)$. Because this point is in the image of \mathbf{A}_V , there must exist a point $\mathbf{c} \in \mathbb{R}^{|V|}$ such that $\mathbf{z} = \mathbf{A}_V \mathbf{c}$. Now we evaluate

$$\hat{r}(\mathbf{z}) = \mathbf{R} \mathbf{z} = \mathbf{R} \mathbf{A}_V \mathbf{c} \quad (25)$$

$$= \mathbf{L}^{-1} \mathbf{c} \quad (26)$$

$$= \mathbf{L}^{-1} \mathbf{A}_V^+ \mathbf{A}_V \mathbf{c} \quad (27)$$

$$= \mathbf{L}^{-1} \mathbf{A}_V^+ \mathbf{z}, \quad (28)$$

where we used the fact $\mathbf{R} \mathbf{A}_V = \mathbf{L}^{-1}$ in Eqn. (26) and the fact that $\mathbf{A}_V^+ \mathbf{A}_V = \mathbf{I}$ in Eqn. (27). This concludes the proof. \square

A.3. Proof of Prop. 3 (permutation identifiability)

The proof is heavily based on Lachapelle et al. (2023) and Xu et al. (2024).

Proposition 3 (Identifiability up to permutation). *Suppose (\hat{r}, \hat{q}) is a solution to the constrained problem of Eqns. (4) and (5) with $\beta = \mathbb{E} \|\delta_V^c\|_0$. Under Asm. 1 to 4, there exists an invertible diagonal matrix and a permutation matrix $\mathbf{D}, \mathbf{P} \in \mathbb{R}^{|V| \times |V|}$ such that $\hat{q} = \mathbf{A}_V \mathbf{D} \mathbf{P}$ and $\hat{r}(\mathbf{z}) = \mathbf{P}^T \mathbf{D}^{-1} \mathbf{A}_V^+ \mathbf{z}$ for all $\mathbf{z} \in \text{Im}(\mathbf{A}_V)$, where $\text{Im}(\mathbf{A}_V)$ is the image of \mathbf{A}_V .*

Proof. Recall that, in the proof of Prop. 2, we showed that the solution $q^* := \mathbf{A}_V$ and $r^* := \mathbf{A}_V^+$ yields zero reconstruction loss, i.e.,

$$\mathbb{E}_{\mathbf{x}, \bar{\mathbf{x}}} \|\delta^z - q^*(r^*(\delta^z))\|_2^2 = 0. \quad (29)$$

It turns out, this solution also satisfies the constraint $\mathbb{E}\|r(\delta^z)\|_0 \leq \beta := \mathbb{E}\|\delta_V^c\|_0$ since

$$\mathbb{E}\|r^*(\delta^z)\|_0 = \mathbb{E}\|\mathbf{A}_V^+(\mathbf{A}_V\delta_V^c)\|_0 = \mathbb{E}\|\delta_V^c\|_0 = \beta, \quad (30)$$

where we used the fact that $\delta^z = \mathbf{A}_V\delta_V^c$ and $\mathbf{A}_V^+\mathbf{A}_V = \mathbf{I}$, since \mathbf{A}_V is injective. This means that all optimal solutions to the constrained problem of Eqns. (4) and (5) with $\beta := \mathbb{E}\|\delta_V^c\|_0$ must reach zero reconstruction loss.

Let (\hat{r}, \hat{q}) be an arbitrary solution to the constrained problem. By the above argument, this solution must reach zero loss. Thus, by the exact same argument as in Prop. 2, there must exist an invertible matrix $\mathbf{L} \in \mathbb{R}^{|V| \times |V|}$ such that

$$\hat{q} := \mathbf{A}_V\mathbf{L} \quad \text{and} \quad \hat{r}(\mathbf{z}) := \mathbf{L}^{-1}\mathbf{A}_V^+\mathbf{z}, \quad \text{for all } \mathbf{z} \in \text{Im}(\mathbf{A}_V). \quad (31)$$

Since \hat{r} is optimal it must satisfy the constraint, which we rewrite as

$$\begin{aligned} \mathbb{E}\|\hat{r}(\delta^z)\|_0 &\leq \mathbb{E}\|\delta_V^c\|_0 \\ \mathbb{E}\|\hat{r}(\mathbf{A}_V\delta_V^c)\|_0 &\leq \mathbb{E}\|\delta_V^c\|_0 \\ \mathbb{E}\|\mathbf{L}^{-1}\mathbf{A}_V^+(\mathbf{A}_V\delta_V^c)\|_0 &\leq \mathbb{E}\|\delta_V^c\|_0 \\ \mathbb{E}\|\mathbf{L}^{-1}\delta_V^c\|_0 &\leq \mathbb{E}\|\delta_V^c\|_0, \end{aligned} \quad (32)$$

where we used the fact that \hat{r} restricted to the image of \mathbf{A}_V is equal to $\mathbf{L}^{-1}\mathbf{A}_V^+$ when going from the second to the third line.

At this stage, we can use the same argument as Lachapelle et al. (2023) to conclude that \mathbf{L} is a permutation-scaling matrix. For completeness, we present that result into Lemma 4 and its proof below. One can directly apply this lemma, thanks to Asm. 4 and the fact that sets of the form $\{\delta_S^c \in \mathbb{R}^{|V|} \mid \mathbf{a}^\top \delta_S^c = 0\}$ with $\mathbf{a} \neq 0$ are proper linear subspaces of $\mathbb{R}^{|V|}$ and thus have zero Lebesgue measure, and thus

$$\mathbb{P}_{\delta_S^c|S}\{\delta_S^c \in \mathbb{R}^{|V|} \mid \mathbf{a}^\top \delta_S^c = 0\} = 0.$$

This concludes the proof. \square

The proof of the following lemma is taken directly from Lachapelle et al. (2023) (modulo minor changes in notation). The original work used this argument inside a longer proof and did not encapsulate this result into a modular lemma. We thus believe it is useful to restate the result here as a lemma containing only the piece of the argument we need. We also include the proof of Lachapelle et al. (2023) for completeness. Note that Xu et al. (2024) also reused this result to prove identifiability up to permutation and scaling.

Lemma 4 (Lachapelle et al. (2023)). *Let $\mathbf{L} \in \mathbb{R}^{m \times m}$ be an invertible matrix and let \mathbf{x} be an m -dimensional random vector following some distribution $\mathbb{P}_{\mathbf{x}}$. Define the set $S := \{j \in [m] \mid \mathbf{x}_j \neq 0\}$, which is random (because \mathbf{x} is random) with probability mass function given by $p(S)$. Let $\mathcal{S} := \{S \subseteq [m] \mid p(S) > 0\}$, i.e. it is the support of $p(S)$. Assume that*

1. *For all $j \in [m]$, we have $\bigcup_{S \in \mathcal{S} \mid j \notin S} S = [m] \setminus \{j\}$; and*
2. *For all $S \in \mathcal{S}$, the conditional distribution $\mathbb{P}_{\mathbf{x}_S|S}$ is such that, for all nonzero $\mathbf{a} \in \mathbb{R}^{|S|}$, $\mathbb{P}_{\mathbf{x}_S|S}\{\mathbf{x}_S \mid \mathbf{a}^\top \mathbf{x}_S = 0\} = 0$.*

Under these assumptions, if $\mathbb{E}\|\mathbf{L}\mathbf{x}\|_0 \leq \mathbb{E}\|\mathbf{x}\|_0$, then \mathbf{L} is a permutation-scaling matrix, i.e. there exists a diagonal matrix \mathbf{D} and a permutation matrix \mathbf{P} such that $\mathbf{L} = \mathbf{D}\mathbf{P}$

Proof. We start by rewriting the l.h.s. of $\mathbb{E}\|\mathbf{L}\mathbf{x}\|_0 \leq \mathbb{E}\|\mathbf{x}\|_0$ as

$$\mathbb{E}\|\mathbf{x}\|_0 = \mathbb{E}_{p(S)}\mathbb{E}\left[\sum_{j=1}^m \mathbf{1}(\mathbf{x}_j \neq 0) \mid S\right] \quad (33)$$

$$= \mathbb{E}_{p(S)}\sum_{j=1}^m \mathbb{E}[\mathbf{1}(\mathbf{x}_j \neq 0) \mid S] \quad (34)$$

$$= \mathbb{E}_{p(S)}\sum_{j=1}^m \mathbb{P}_{\mathbf{x}|S}\{\mathbf{x} \in \mathbb{R}^m \mid \mathbf{x}_j \neq 0\} \quad (35)$$

$$= \mathbb{E}_{p(S)}\sum_{j=1}^m \mathbf{1}(j \in S), \quad (36)$$

where the last step follows from the definition of S .

Moreover, we rewrite $\mathbb{E}\|\mathbf{L}\mathbf{x}\|_0$ as

$$\mathbb{E}\|\mathbf{L}\mathbf{x}\|_0 = \mathbb{E}_{p(S)} \mathbb{E} \left[\sum_{j=1}^m \mathbf{1}(\mathbf{L}_{j,:} \mathbf{x} \neq 0) \mid S \right] \quad (37)$$

$$= \mathbb{E}_{p(S)} \sum_{j=1}^m \mathbb{E}[\mathbf{1}(\mathbf{L}_{j,:} \mathbf{x} \neq 0) \mid S] \quad (38)$$

$$= \mathbb{E}_{p(S)} \sum_{j=1}^m \mathbb{E}[\mathbf{1}(\mathbf{L}_{j,S} \mathbf{x}_S \neq 0) \mid S] \quad (39)$$

$$= \mathbb{E}_{p(S)} \sum_{j=1}^m \mathbb{P}_{\mathbf{x}|S} \{ \mathbf{x} \in \mathbb{R}^m \mid \mathbf{L}_{j,S} \mathbf{x}_S \neq 0 \}. \quad (40)$$

Notice that

$$\mathbb{P}_{\mathbf{x}|S} \{ \mathbf{x} \in \mathbb{R}^m \mid \mathbf{L}_{j,S} \mathbf{x}_S \neq 0 \} = 1 - \mathbb{P}_{\mathbf{x}|S} \{ \mathbf{x} \in \mathbb{R}^m \mid \mathbf{L}_{j,S} \mathbf{x}_S = 0 \}. \quad (41)$$

Define N_j be the support of $\mathbf{L}_{j,:}$, i.e., $N_j := \{i \in [m] \mid \mathbf{L}_{j,i} \neq 0\}$.

When $S \cap N_j = \emptyset$, we have that $\mathbf{L}_{j,S} = \mathbf{0}$ and thus

$$\mathbb{P}_{\mathbf{x}|S} \{ \mathbf{x} \in \mathbb{R}^m \mid \mathbf{L}_{j,S} \mathbf{x}_S = 0 \} = 1.$$

When $S \cap N_j \neq \emptyset$, we have that $\mathbf{L}_{j,S} \neq \mathbf{0}$, and thus, by the second assumption, we have that

$$\mathbb{P}_{\mathbf{x}|S} \{ \mathbf{x} \in \mathbb{R}^m \mid \mathbf{L}_{j,S} \mathbf{x}_S = 0 \} = 0.$$

Thus we can write

$$\mathbb{P}_{\mathbf{x}|S} \{ \mathbf{x} \in \mathbb{R}^m \mid \mathbf{L}_{j,S} \mathbf{x}_S \neq 0 \} = 1 - \mathbb{P}_{\mathbf{x}|S} \{ \mathbf{x} \in \mathbb{R}^m \mid \mathbf{L}_{j,S} \mathbf{x}_S = 0 \} \quad (42)$$

$$= 1 - \mathbf{1}(S \cap N_j = \emptyset) \quad (43)$$

$$= \mathbf{1}(S \cap N_j \neq \emptyset), \quad (44)$$

which allows us to write

$$\mathbb{E}\|\mathbf{L}\mathbf{x}\|_0 = \mathbb{E}_{p(S)} \sum_{j=1}^m \mathbf{1}(S \cap N_j \neq \emptyset). \quad (45)$$

The original inequality $\mathbb{E}\|\mathbf{L}\mathbf{x}\|_0 \leq \mathbb{E}\|\mathbf{x}\|_0$ can thus be rewritten as

$$\mathbb{E}_{p(S)} \sum_{j=1}^m \mathbf{1}(S \cap N_j \neq \emptyset) \leq \mathbb{E}_{p(S)} \sum_{j=1}^m \mathbf{1}(j \in S). \quad (46)$$

Since \mathbf{L} is invertible, there exists a permutation $\sigma : [m] \rightarrow [m]$ such that, for all $j \in [m]$, $\mathbf{L}_{j,\sigma(j)} \neq 0$ (e.g. see Lemma B.1 from [Lachapelle et al. \(2023\)](#)). In other words, for all $j \in [m]$, $j \in N_{\sigma(j)}$. Of course we can permute the terms of the l.h.s. of Eqn. (46), which yields

$$\mathbb{E}_{p(S)} \sum_{j=1}^m \mathbf{1}(S \cap N_{\sigma(j)} \neq \emptyset) \leq \mathbb{E}_{p(S)} \sum_{j=1}^m \mathbf{1}(j \in S) \quad (47)$$

$$\mathbb{E}_{p(S)} \sum_{j=1}^m (\mathbf{1}(S \cap N_{\sigma(j)} \neq \emptyset) - \mathbf{1}(j \in S)) \leq 0. \quad (48)$$

We notice that each term $\mathbf{1}(S \cap N_{\sigma(j)} \neq \emptyset) - \mathbf{1}(j \in S) \geq 0$ since whenever $j \in S$, we also have that $j \in S \cap N_{\sigma(j)}$ (recall $j \in N_{\sigma(j)}$). Thus, the l.h.s. of Eqn. (48) is a sum of non-negative terms which is itself non-positive. This means that every term in the sum is zero:

$$\forall S \in \mathcal{S}, \forall j \in [m], \mathbf{1}(S \cap N_{\sigma(j)} \neq \emptyset) = \mathbf{1}(j \in S). \quad (49)$$

Importantly,

$$\forall j \in [m], \forall S \in \mathcal{S}, j \notin S \implies S \cap N_{\sigma(j)} = \emptyset, \quad (50)$$

and since $S \cap N_{\sigma(j)} = \emptyset \iff N_{\sigma(j)} \subseteq S^c$ we have that

$$\forall j \in [m], \forall S \in \mathcal{S}, j \notin S \implies N_{\sigma(j)} \subseteq S^c \quad (51)$$

$$\forall j \in [m], N_{\sigma(j)} \subseteq \bigcap_{S \in \mathcal{S} | j \notin S} S^c. \quad (52)$$

By assumption, we have $\bigcup_{S \in \mathcal{S} | j \notin S} S = [m] \setminus \{j\}$. By taking the complement on both sides and using De Morgan's law, we get $\bigcap_{S \in \mathcal{S} | j \notin S} S^c = \{j\}$, which implies that $N_{\sigma(j)} = \{j\}$ by Eqn. (52). Thus, $\mathbf{L} = \mathbf{D}\mathbf{P}$ where \mathbf{D} is an invertible diagonal matrix and \mathbf{P} is a permutation matrix. \square

A.4. Distributions satisfying Asm. 4

In $\mathbb{R}^{|S|}$, any lower-dimensional subspace has Lebesgue measure 0. By defining the probability measure of $\delta_S^c | S$ with respect to the Lebesgue measure, its integral over any lower-dimensional subspace of $\mathbb{R}^{|S|}$ will be 0. Consider a few examples of $\mathbb{P}_{\delta_S^c | S}$ directly taken from (Lachapelle et al., 2023) with adapted notation just for illustration purposes.

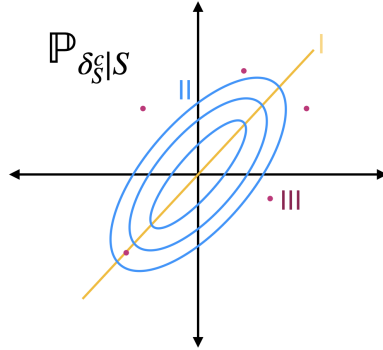


Figure 4: Three illustrative examples of $\mathbb{P}_{\delta_S^c | S}$: Only distribution II satisfies Asm. 4.

In Figure 4, distributions I and III do not satisfy Asm. 4 whereas distribution II does. This is because I represents the support of a Gaussian distribution with a low-rank covariance and III represents finite support; both of these distributions will be measure zero in $\mathbb{R}^{|S|}$. On the other hand, II represents level sets of a Gaussian distribution with full-rank covariance. Please refer to Lachapelle et al. (2023) for a comprehensive explanation.

A.5. Interpreting the Linear Representation Hypothesis

Corollary 5. *If concept changes act on latent embeddings following $\tilde{\mathbf{z}} = \mathbf{z} + \delta^z$ and q and r are injective, they must be affine transformations.*

Proof: Starting with the interpretation of the *linear representation hypothesis* such that $\tilde{\mathbf{z}} = \mathbf{z} + \delta^z$ where $\mathbf{z} = q(\mathbf{c})$ and $\tilde{\mathbf{z}} = q(\tilde{\mathbf{c}})$:

$$\implies q(\tilde{\mathbf{c}}) = q(\mathbf{c}) + \delta^z$$

Since we identify only the varying concepts, this corresponds to identifying a subspace of the original concept space in which $\tilde{\mathbf{c}} = \mathbf{c} + \delta_V^c$.

Using the injectivity of q (Asm. 2):

$$q(\mathbf{c} + \delta_V^c) = q(\mathbf{c}) + \delta^z \quad (53)$$

Taking the gradient of both the LHS and the RHS wrt \mathbf{c} ,

$$\begin{aligned} \frac{\partial(\mathbf{c} + \delta_V^c)}{\partial(\mathbf{c})} \nabla_{(\mathbf{c} + \delta_V^c)} q(\mathbf{c} + \delta_V^c) &= \nabla_{\mathbf{c}} q(\mathbf{c}) \\ \nabla_{(\mathbf{c} + \delta_V^c)} q(\mathbf{c} + \delta_V^c) &= \nabla_{\mathbf{c}} q(\mathbf{c}) \\ \mathbf{J}^T(\mathbf{c} + \delta_V^c) &= \mathbf{J}^T(\mathbf{c}) \end{aligned} \quad (54)$$

Where $\mathbf{J}(\mathbf{c})$ is the Jacobian of q at \mathbf{c} and $\mathbf{J}(\mathbf{c} + \delta_V^c)$ is the Jacobian of q at $\mathbf{c} + \delta_V^c$.

$$\begin{bmatrix} \nabla q_1(\mathbf{c} + \delta_V^c) \\ \nabla q_2(\mathbf{c} + \delta_V^c) \\ \nabla q_3(\mathbf{c} + \delta_V^c) \\ \vdots \\ \nabla q_{dz}(\mathbf{c} + \delta_V^c) \end{bmatrix} - \begin{bmatrix} \nabla q_1(\mathbf{c}) \\ \nabla q_2(\mathbf{c}) \\ \nabla q_3(\mathbf{c}) \\ \vdots \\ \nabla q_{dz}(\mathbf{c}) \end{bmatrix} = 0$$

considering the j^{th} component of the difference,

$$\begin{bmatrix} \nabla^2 q_j(\theta_1) \\ \nabla^2 q_j(\theta_2) \\ \nabla^2 q_j(\theta_2) \\ \vdots \\ \nabla^2 q_j(\theta_d) \end{bmatrix} (\delta_V^c) = 0$$

Following the proof in (Ahuja et al., 2022), $\nabla^2 q_j(\mathbf{c}) = 0$, which implies $q(\mathbf{c}) = \mathbf{A}_V \mathbf{c} + \mathbf{b}$ where $\mathbf{A}_V \in \mathbb{R}^{d_z \times d_z}$, $\mathbf{b} \in \mathbb{R}^{d_z}$ or that q is affine. Similarly, we can show that r is affine too by starting with $r(\mathbf{z} + \delta^z) = r(\mathbf{z}) + \delta_V^c$.

Corollary 6. *If we assume $\tilde{\mathbf{z}} = \phi(\mathbf{z})$, for an affine map q , $\mathbf{A} = \mathbf{I}$.*

Proof: Let's assume the affine form of q can be expressed as:

$$\mathbf{z} = \mathbf{A}_V \mathbf{c} + \mathbf{b} \quad (55)$$

where $\mathbf{A}_V \in \mathbb{R}^{d_z \times d_z}$ and $\mathbf{b} \in \mathbb{R}^{d_z}$.

Similarly, $\tilde{\mathbf{z}} = q(\tilde{\mathbf{c}}) = \mathbf{A}_V \tilde{\mathbf{c}} + \mathbf{b}$ and we know $\tilde{\mathbf{c}} = \mathbf{c} + \delta_V^c$.

$$\implies \tilde{\mathbf{z}} = \mathbf{A}_V(\mathbf{c} + \delta_V^c) + \mathbf{b}$$

we have $\tilde{\mathbf{z}} = \phi(\mathbf{z})$ and from Eqn. (55):

$$\phi(\mathbf{A}_V \mathbf{c} + \mathbf{b}) = \mathbf{A}_V(\mathbf{c} + \delta_V^c) + \mathbf{b} \quad (56)$$

In the above equation, we can see that the maximum degree of \mathbf{c} on the RHS is 1, which implies that the degree of \mathbf{c} on the LHS should also at most be 1, which implies ϕ can at most be an affine function.

So let's assume ϕ is an affine function of the form:

$$\tilde{\mathbf{z}} = \phi(\mathbf{z}) = \mathbf{T}\mathbf{z} + \delta^z \quad (57)$$

where $\mathbf{T} \in \mathbb{R}^{d_z \times d_z}$ and $\delta^z \in \mathbb{R}^{d_z}$. Substituting this in the above equation, we get:

$$\begin{aligned} \mathbf{T}(\mathbf{A}_V \mathbf{c} + \mathbf{b}) + \delta^z &= \mathbf{A}_V(\mathbf{c} + \delta_V^c) + \mathbf{b} \\ \mathbf{Q}(\mathbf{T} - \mathbf{I})\mathbf{c} + (\mathbf{T} - \mathbf{I})\mathbf{b} + (\delta^z - \mathbf{Q}\delta_V^c) &= 0 \end{aligned} \quad (58)$$

For a non-trivial solution:

$$\mathbf{T} = \mathbf{I} \quad (59)$$

$$\delta^z = \mathbf{A}_V \delta_V^c \quad (60)$$

So, we have proved that if we assume q to be affine, then $\tilde{\mathbf{z}} = \mathbf{z} + \delta\mathbf{z}$.

Implications: Multiple expositions (Templeton et al., 2024) remark that it is not clear what the meaning of *linear* exactly is in the linear representation hypothesis. Informally, many results cited in support of the linear representation hypothesis either extract information with a linear probe, or add a vector to influence model behavior. Here, we assume that if linear meant concepts are linearly encoded in the latent space, we can show that this would correspond to shifts in the latent space representing net concept changes and vice versa, which means both interpretations are the same, so it does not matter which one is assumed.

B. Implementation and experimental details

B.1. SSAE Architecture

The encoding $r : \mathcal{Z} \rightarrow \mathcal{C}$ and decoding functions $q : \mathcal{C} \rightarrow \mathcal{Z}$ constituting the SSAE autoencoding framework are parameterized as follows:

$$\hat{\delta}_V^c := r(\delta^z) := \mathbf{W}_e(\delta^z - \mathbf{b}_d) + \mathbf{b}_e; \quad (61)$$

$$\hat{\delta}^z := q(\hat{\delta}_V^c) := \mathbf{W}_d \hat{\delta}_V^c + \mathbf{b}_d. \quad (62)$$

Parameters. $\mathbf{W}_e \in \mathbb{R}^{|V| \times d_z}$, $\mathbf{b}_e \in \mathbb{R}^{|V|}$, $\mathbf{W}_d \in \mathbb{R}^{d_z \times |V|}$, and $\mathbf{b}_d \in \mathbb{R}^{d_z}$ denote the encoder weights, encoder bias, decoding weights, and decoder bias respectively. The decoder bias is also treated as a pre-encoder bias purely for empirical performance improvement reasons based on ongoing discourse on engineering improvements in SAEs (Bricken et al., 2023; Gao et al., 2024). The encoder and decoder weights are initialised s.t. $\mathbf{W}_d = \mathbf{W}_e^T$. The bias terms \mathbf{b}_e and \mathbf{b}_d are initialised to be all zero vectors. Further, after every iteration, the columns of \mathbf{W}_d are unit normalised following Bricken et al. (2023); Gao et al. (2024).

Data. Data is layer-normalised analogous to Gao et al. (2024) prior to being passed as input to the encoder in batch sizes of 32.

Optimization. Specifically, the following objective is optimized:

$$\min \frac{1}{N} \sum_{i=1}^N \frac{\|\delta_{(i)}^z - q(r(\delta_{(i)}^z))\|_2^2}{\|\delta_{(i)}^z\|_2^2}, \quad (63)$$

$$\text{s.t. } \frac{1}{|V|N} \sum_{i=1}^N \|r(\delta_{(i)}^z)\|_1 \leq \beta \quad (64)$$

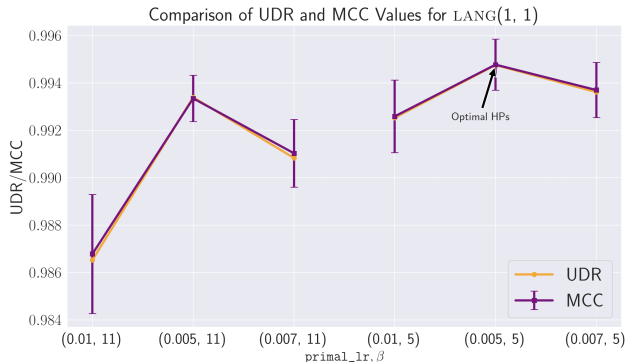


Figure 5: UDR scores suggest a `primal_lr` value of 0.005 and a β value of 5.

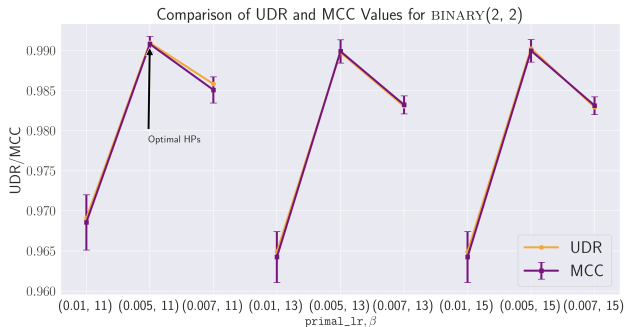


Figure 6: UDR scores suggest a `primal_lr` value of 0.005 and a β value of 11.

We optimize the above constrained minimisation problem by computing its Lagrangian and the primal and dual gradients using the `cooper` library (Gallego-Posada & Ramirez, 2022). We use ExtraAdam (Gidel et al., 2020) as both the primal and the dual optimizer, with the values of the primal and dual learning rates fixed throughout training and selected based on UDR scores (see Apx. B.1.1). ExtraAdam uses *extrapolation from the past* to provide similar convergence properties as extra-gradient optimizers (Korpelevich, 1976) without requiring twice as many gradient computations per parameter update or auxiliary storage of trainable parameters (Gidel et al., 2020; Gallego-Posada & Ramirez, 2022). Further, to account for the unit-norm adjustment of the columns of the decoder weights \mathbf{W}_d , we adjust gradients to remove discrepancies between the true gradients and the ones used by the optimizer. This done by removing any gradient information parallel to the columns of \mathbf{W}_d at every step after the normalisation of the columns of \mathbf{W}_d .

B.1.1. MODEL SELECTION VIA UNSUPERVISED DIVERSITY RANKING (UDR)

Unsupervised model selection remains a notoriously difficult problem since there appears to be no unsupervised way of distinguishing between bad and good random seeds; unsupervised model selection should not depend on ground truth labels since these might biased the results based on supervised metrics. Moreover, in disentanglement settings, hyperparameter selection cannot rely solely on choosing the best validation-set performance. This is because there is typically a trade-off between the quality of fit and the degree of disentanglement ((Locatello et al., 2019), Sec 5.4). For the proposed method in Section 2.4, identifiability of the decoder and of the learnt representation is essential to recover steering vectors for individual concepts. It is possible that a decoder with higher reconstruction error is identified to a greater degree. Hence, it is not sufficient to engineer a good unsupervised model solely based on how well it minimizes the reconstruction loss. Duan et al. (2019) propose the Unsupervised Disentanglement Ranking (UDR) score (Duan et al., 2019), which measures the consistency of the model across different initial weight configurations (seeds), which we use to fit our model. It is calculated as follows: for every hyperparameter setting, we compute MCCs between pairs of different runs and compute the median of all pairwise MCCs as the UDR score. We report the UDR scores and the mean pair-wise MCCs for the two most important hyperparameters affecting observed reconstruction error and MCC values—the learning rate of the primal optimizer (`primal_lr`) and the sparsity level (β)—over 10 pairs of 5 random seeds in Figure 5 for the dataset,

LANG(1, 1), and in Figure 6 for BINARY(2, 2), over a selected hyperparameter range corresponding to decent reconstruction error. At slightly different hyperparameter settings, reconstruction error may spike even if the MCC remains acceptable. Such scenarios often fall outside the scope of consideration here, as they break the assumption of near-perfect reconstruction. While models may not achieve zero reconstruction loss in practice, we still expect it to remain reasonably low. As can be seen in Figure 5 and Figure 6, MCC values typically correlate with the UDR scores. Further, using these different models, we perform a sensitivity analysis on the two most important hyperparameters of our model—the sparsity level ϵ and the learning rate, which we report in Apx. B.4.

B.1.2. SPARSE OPTIMIZATION

We choose to enforce sparsity in the learning objective of the model as an explicit constraint rather than as l_1 -regularisation due to the benefits listed in Table 4. In areas such as compressive sensing, signal processing, and certain machine learning applications, constrained optimization approaches have shown superior performance in recovering sparse signals and providing better generalization performance.

	Constrained optimization	l_1 -regularisation
<i>Optimization efficiency</i>	Finding the optimal solution and enforcing sparsity are separate tasks. Methods like augmented Lagrangian formulations iteratively enforce sparsity while optimizing the objective function, which can lead to more stable convergence.	The l_1 penalty introduces a non-differentiable point at zero, which requires careful tuning and can be sensitive to initialization and hyperparameters.
<i>Hyperparameter tuning</i>	The primary hyperparameter is the sparsity level ϵ , which can be set based on domain knowledge or practical constraints, simplifying the model selection process.	The primary hyperparameter is the strength of the sparsity penalty in the training objective λ , which needs tuning to prevent under or over-fitting.
<i>Interpretability and control</i>	We have precise control on the sparsity of the solution since the relationship between ϵ and solution sparsity is direct. The solution is easier to interpret.	The relationship between λ and the resulting solution sparsity is complex and non-linear and a small change in the value of λ can lead to very large solution changes, making it difficult to control or interpret.

Table 4: Benefits of constrained optimization over regularisation for enforcing sparsity.

B.1.3. DATASETS

We list out data generation pipelines for the semi-synthetic datasets in Figure 7 and Figure 8 and refer the reader to (Lin et al., 2022) and the corresponding Hugging Face repository for details on the multiple-choice subset of TruthfulQA considered in this paper.

B.1.4. MEAN CORRELATION COEFFICIENT: GATEWAY TO INTERPRETING LATENT DIMENSIONS

In modern work on identifiable representation learning, the Mean Correlation Coefficient (MCC) was proposed to be used as a metric by Hyvarinen & Morioka (2016) to evaluate the recovery of true source signals through their estimates. It was further developed as a metric by Khemakhem et al. (2020b) to measure on an average how well the elements of two vectors $\mathbf{x} \in \mathbb{R}^n$ and $\mathbf{y} \in \mathbb{R}^n$ are correlated under the best possible alignment of their ordering, i.e., MCC measures the average maximum correlation that can be achieved when each variable x_i from \mathbf{x} is paired with a variable y_j from \mathbf{y} across all possible permutations of such pairings, i.e, across $(i, \pi(j))$ where $\pi \in S_n$, the set of all permutations of the n indices.

To understand the steps involved in computing this metric, let $\mathbf{x} = (x_1, x_2)$ and $\mathbf{y} = (y_1, y_2)$ be two bivariate random variables. Then,

LANG(1, 1)

Generate pairs of text samples varying only in their language, within a pair and having the same type of variation in language across all pairs. Choosing *eng* → *french* as the variation in the concept of *language*, so as to learn the steering vector *eng* → *french*, we generate pairs of words describing common *household objects*, such as:

```
[("Door", "Porte"), ("Dog", "Chien"), ("Shirt", "Chemise"), ("fish", "poisson"), ("Pillow", "Oreiller"), ("Blanket", "Couverture"), ("Sunday", "Dimanche"), ("Hat", "Chapeau"), ("Umbrella", "Parapluie"), ("Glasses", "Lunettes"), ("Clock", "Horloge"), ...]
```

GENDER(1, 1)

Generate pairs of text samples varying only in gender within a pair and having the same type of variation in gender across all pairs. Choosing *masculine* → *feminine* as the variation in the concept of *gender*, so as to learn the steering vector *masculine* → *feminine*, we generate pairs of words describing common *professions*, such as:

```
[("grandpa", "grandma"), ("grandson", "granddaughter"), ("groom", "bride"), ("he", "she"), ("headmaster", "headmistress"), ("heir", "heiress"), ("hero", "heroine"), ("husband", "wife"), ("king", "queen"), ("lion", "lioness"), ("man", "woman"), ("manager", "manageress"), ("men", "women"), ...]
```

BINARY(2, 2)

Generate pairs of text samples varying in *gender* and *language* such that it is not known if which of the two, or both, vary within any pair. Choosing *masculine* → *feminine* as the variation in the concept of *gender* and *eng* → *french* as the variation in the concept of *language*, so as to learn the steering vectors for *masculine* → *feminine* and *eng* → *french*, we generate pairs of words describing common *professions*, such as:

```
[("brother", "sister"), ("buck", "doe"), ("bull", "cow"), ("daddy", "mommy"), ("fils", "fille"), ("homme", "femme"), ("mari", "femme"), ("acteur", "actrice"), ("Duc", "Duchess"), ("Widow", "Veuf"), ("Taureau", "Cow"), ("Hen", "Coq"), ...]
```

Here, we generate an equal number of samples with only *masculine* → *feminine*, only *eng* → *french*, and both *masculine* → *feminine* and *eng* → *french* variations.

CORR(2, 1)

Generate pairs of text samples varying only in language within a pair but having two different types of variation in language across all pairs. Choosing *eng* → *french* and *eng* → *german* as the two types of variations in the concept of *language*, so as to learn the steering vector *eng* → *french*, we generate pairs of words describing common *professions*, such as:

```
[("Doctor", "arzt"), ("Lehrer", "teacher"), ("Engineer", "Ingenieur"), ("Pflegefachkraft", "Nurse"), ("headmaster", "headmistress"), ("Teacher", "Enseignant"), ("Infirmier", "Nurse"), ("Koch", "Chef"), ...]
```

Generate an equal number of pairs for each variation *eng* → *german* and *eng* → *french* with correlated pairs.

Figure 7: Data generation pipeline for semi-synthetic language datasets considering binary contrasts in underlying concepts from a potentially higher-level concept consisting of several such binary contrasts.

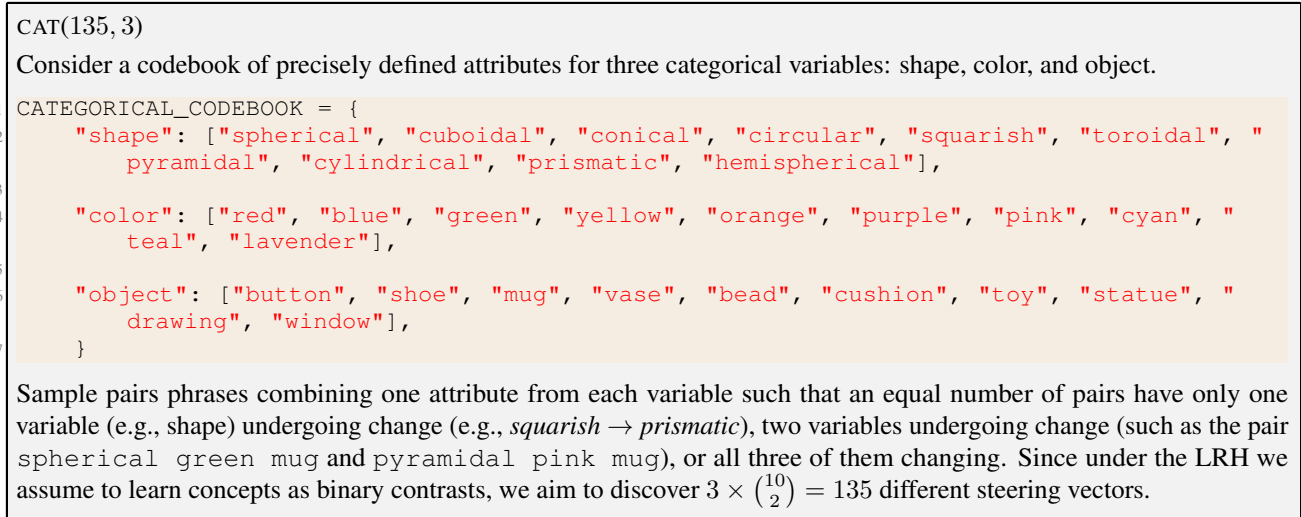


Figure 8: Data generation pipeline for a significantly harder dataset than the ones in Figure 7 considering explicitly categorical variables and their attributes to learn steering vectors for corresponding binary contrasts.

- Append \mathbf{y} to \mathbf{x} , treating rows as observations and the columns as variables (i.e. $[x_1, x_2, y_1, y_2]$).
- Compute absolute values of the Pearson correlation coefficients between \mathbf{x} and \mathbf{y} , yielding the following matrix:

$$\begin{bmatrix} \text{abs}(\text{corr}(x_1, y_1)) & \text{abs}(\text{corr}(x_1, y_2)) \\ \text{abs}(\text{corr}(x_2, y_1)) & \text{abs}(\text{corr}(x_2, y_2)) \end{bmatrix}.$$
- Next, solve the linear sum assignment problem to select the absolute correlation coefficients for pairings between components of \mathbf{x} and \mathbf{y} such that the sum of the selected coefficients is maximised. Operationally, if the pairing is of x_1 with y_1 , this corresponds to a pairing score of $\text{abs}(\text{corr}(x_1, y_1)) + \text{abs}(\text{corr}(x_2, y_2))$. The only other possible pairing in this case would have a score of $\text{abs}(\text{corr}(x_1, y_1)) + \text{abs}(\text{corr}(x_2, y_2))$. Select the maximum of the scores of these pairings.
- The MCC value then would be the mean of the correlation coefficients of the optimal pairings. For example, if the best pairings are (x_1, y_1) and (x_2, y_2) , then MCC would be $\text{mean}(\text{abs}(\text{corr}(x_1, y_1)), \text{abs}(\text{corr}(x_2, y_2)))$.

Evaluating learnt representations. When the ground truth latent representation is known, MCC is computed between the ground truth variable and its estimate. When the ground truth is unknown, MCC is computed by comparing pairs of latent representations, where each stems from a different random initialisation of the representation learner. This tests if the model can consistently learn representations within the equivalence class of permutation and scaling.

Why consider permutations? It is essential to consider all permutations between the variables \mathbf{x} and \mathbf{y} to maximise the average correlation between them since it is possible that the average correlation for a pair of perfectly correlated variables is 0. To observe this, consider an example reproduced from (Khemakhem et al., 2020b): Where $\mathbf{x} = (x_1, x_2)$ s.t. $x_1 \perp x_2$ and $\mathbf{y} = (x_2^2, x_1^2)$. Then $\frac{1}{2} \sum_i \text{corr}(x_i, y_i) = 0$ since $x_1 \perp x_2$ even though \mathbf{x} completely determines \mathbf{y} . Moreover, since it is not possible to resolve indeterminacies up to permutation and rescaling in recovering variables, it is important to consider different orderings of the components.

Other metrics. While MCC measures permutation-identifiability, other metrics such as the coefficient of determination R^2 can be used to measure linear identifiability by predicting the ground truth latent variables from the learnt latent variables. The average Pearson correlation between the ground truth and the learnt latents would correspond to the coefficient of multiple correlation (R). $\text{MCC} \leq R \leq R^2$. So measuring MCC values gives us a more conservative estimate for our results. Moreover, MCC allows for other measures of correlations to be considered between the variables, including ones that measure non-linear dependencies such as the Randomised Dependence Coefficient (Lopez-Paz et al., 2013).

B.2. Cosine Similarity

Cosine similarity reflects the geometry of an LLM’s latent space in general, thereby acting as a measure of semantic similarity between embeddings. This is because gradient descent often shapes the latent space of an LLM toward a Euclidean-like

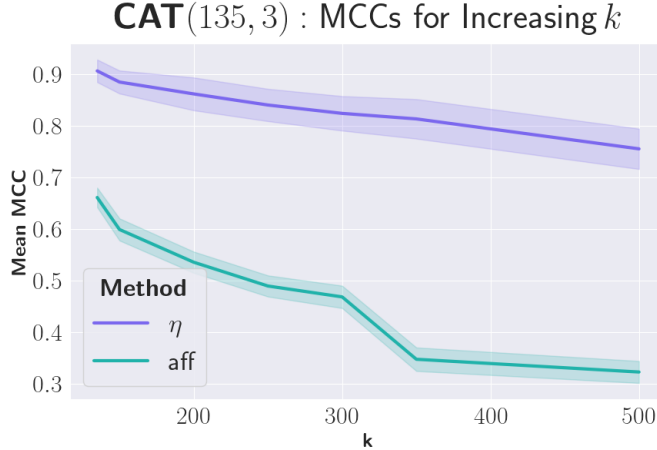


Figure 9: MCC values decrease with an increasing k more sharply for the **aff** baseline.

structure (Jiang et al., 2024), despite it being unidentified by standard pre-training objectives (Park et al., 2023). Further, for the Llama family of models (Llama Team et al., 2024), it has been shown that cosine similarity indeed acts similar to the causal inner product in terms of capturing the semantic structure of embeddings (Park et al., 2023). Empirically, cosine similarity is the most common similarity metric for comparing embeddings.

B.3. 2nd Test of robustness: impact of increasing the dimensionality of the encoder’s output

The output of the encoder is predicted as $\hat{\delta}_V^c \in \mathbb{R}^k$, where $k = |V|$. In Figure 9, we investigate the effect of increasing m beyond $|V|$, i.e., increasing the predicted latent dimension, on MCC values obtained on the dataset with the largest latent dimension, CAT(135, 3). SSAE is reasonably disentangled even when the dimension of the concept vectors to be predicted is fairly *misspecified*, whereas the affine baseline’s MCC values drop sharply.

B.4. Synthetic Experiments

In addition to experiments with LLM embeddings which indicate potential for practical utility, we perform experiments with purely synthetic data in which concepts are precisely known and it is possible to evaluate the model against a known ground-truth. As a teaser to appreciate the relevance of synthetic experiments, consider: even if SAEs consistently learn similar concepts, how can we evaluate if the learnt concepts correspond to the concepts encoded in the input data?

We consider $c_1, c_2, \dots, c_{|V|}$ to correspond to individual concepts. For language data, we assumed that there are concepts like “gender” and “truthfulness” and that they would be represented as one hot vectors c_1 and c_2 . However, such concepts are abstract and it is an assumption that the model would represent both c_1 and c_2 atomically whereas it is possible that c_2 is represented by 2 atomic concepts and c_1 by 1. It is not possible to resolve such ambiguities since the ground truth representations of c_1 and c_2 are not known. For the sake of exposition, in purely synthetic data, c_1 and c_2 are precisely and it is possible to evaluate the model against a known ground truth.

Data. For a brief summary of the number of varying concepts within a pair and across all pairs considered, refer to Table 5. In the case of synthetic data, we generate \mathbf{c} and $\bar{\mathbf{c}}$ first to compute $\delta^c := \bar{\mathbf{c}} - \mathbf{c}$, then apply a dense linear transformation \mathbf{L} to δ^c to generate δ^z as $\delta^z = \mathbf{L}\delta^c$. Importantly, towards the generation of \mathbf{c} , we generate zero vectors in $\mathbb{R}^{|V|}$ such that for any given sample, S components are perturbed by samples from a uniform distribution and others remain zero. This is similar to the data generating process in (Anders et al., 2024) and the conditional distribution of δ_S^c satisfies Asm. 4 of having a density with respect to Lebesgue.

Results. We estimate $\hat{\delta}^c$ and compare it against δ^c to verify the degree of identifiability of the learnt concept vectors or encoder representations. Since we have the ground truth here, we compute the MCC between $(\hat{\delta}^c, \delta^c)$ to measure degree of identifiability. Table 6 shows that the proposed method can identify concepts even for higher values of $|V|$ and $\max(|S|)$ against known ground truth data. Synthetic experiments addressing different facets of the identifiability setting we assume can be readily found in prior work on disentangling representations using sparse shifts (Xu et al., 2024; Lachapelle et al.,

Identifiable steering via sparse auto-encoding of multi-concept shifts

Table 5: Datasets comprise of paired observations $(\mathbf{z}, \bar{\mathbf{z}})$ where \mathbf{z} and $\bar{\mathbf{z}}$ vary in concepts $V = \{c_1, c_2, \dots, c_{|V|}\}$ across all pairs, such that for any given pair, the maximum number of varying concepts is $\max(|S|)$. *Nomenclature for semi-synthetic datasets follows the rule: identifier of the dataset indicating why we consider it, followed by $|V|$ and $\max(|S|)$: IDENTIFIER($|V|$, $\max|S|$).*

Dataset	$ V $	$\max(S)$
SYNTH(3, 2)	3	2
SYNTH(4, 3)	4	3
SYNTH(10, 7)	10	7

Table 6: The mean MCC values between the learnt and the ground truth concept vectors are close to 1.

	SSAE	aff
SYNTH(3, 2)	0.999 ± 0.0001	0.873 ± 0.0561
SYNTH(4, 3)	0.999 ± 0.0011	0.835 ± 0.0097
SYNTH(10, 7)	0.993 ± 0.0005	0.769 ± 0.0103

2023).